2 KINEMATIC AND KINETIC MODELING OF A PLANAR MACHINING CENTER

2.1 Introduction

The books by Nikravesh [65] and Haug [66] emphasize the importance of the application of computer-aided analysis techniques to multi-body mechanical systems. This section gives a brief overview of the more important aspects of computer-aided analysis of mechanical systems as highlighted in the introductory chapter of the book by Nikravesh [65].

A mechanical system is defined as a collection of bodies (or links) in which some or all of the bodies can move relative to each other. Furthermore, mechanical systems may range from the very simple to the very complex, and a specific mechanical system may experience either *planar* (two-dimensional) or *spatial* (three-dimensional) motion.

Any mechanical system can be represented *schematically* as a multi-body system where the actual shape or outline of a body may not be of immediate concern in the process of *analysis*. Of primary importance though, are the connectivity of the joints and the physical characteristics of the elements in the system.

The analysis of a mechanical system is an important tool in the *design process*, i.e. the process of determining which physical characteristics are necessary for a mechanical system to perform a prescribed task. Figure 2.1 shows a block diagram of the "analysis branch" called *mechanics*, which is the study of motion, time and forces.

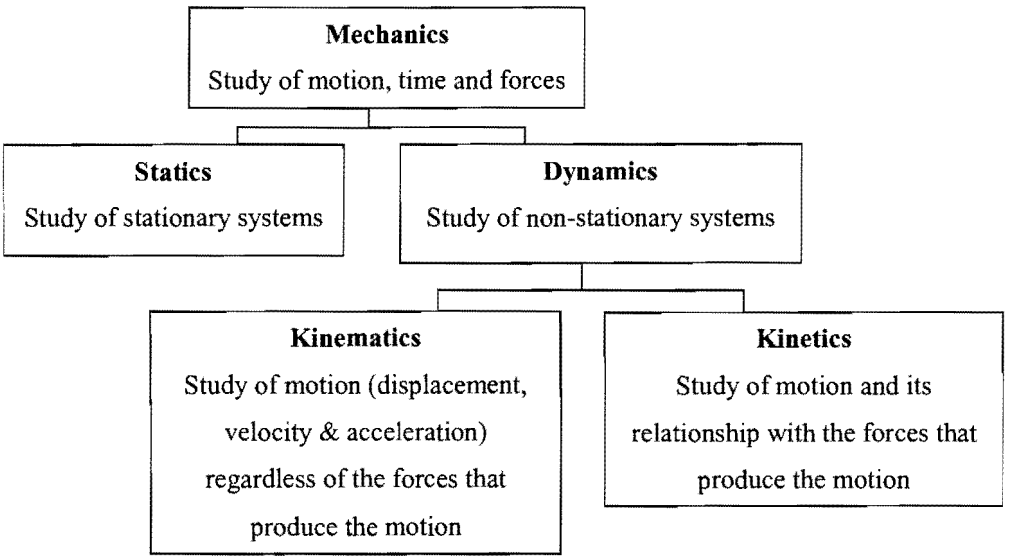

Figure 2.1: Mechanics and its sub-disciplines.

There are two approaches to mechanics: the *graphical approach* and the *analytical approach*. Many classical methods of analysis in mechanics have relied upon graphical and often quite complicated techniques. These techniques are based on geometrical interpretations of the system under consideration. Contrary, the method of solution by vector algebra is an analytical approach, and is more *systematic* when compared to the graphical approach. A problem formulated analytically can be solved repeatedly for different parameter values, a task that is ideally suited to a computer program. The usefulness of writing a computer program becomes even more apparent when the mechanical system under consideration is complex to the extent that, if the system is considered for kinematic analysis, a graphical approach would be very tedious as well as inaccurate.

The purpose of computer-aided analysis of mechanical systems is to develop basic methods for computer formulation and solution of the equations of motion. This requires systematic techniques for formulating the equations and numerical methods for solving them. A computer program for the analysis of mechanical systems can either be a *special-purpose* program or a *general-purpose* program.

A special-purpose program is a rigidly structured computer code that deals with only one type of application. The equations of motion for that particular application are derived a priori and then formulated into the program. As input to the program, the user can provide information such as the dimensions and physical characteristics of each part. Such a program can be made computationally efficient and its storage requirement can be minimized, with the result that it will be suitable for implementation on small personal computers. The major drawback of a special-purpose program is its lack of flexibility for handling other types of applications.

Since the primary interest here is the dynamic analysis of a specific machining center, a special-purpose program is required. The systematic formulation of the relevant equations as applied to the planar machining center, is dealt with in Sections 2.2 – 2.6. The special-purpose computer program that resulted, is tested in Section 2.7.

2.2 Rigid body model

Machining centers are used to control the relative motion between a workpiece and a cutting tool such that the workpiece is shaped into a desired component. The *planar* machining center under consideration consists of a *planar* Gough-Stewart platform with which either the tool or the workpiece can be moved and orientated *in the plane*.

More specifically, the planar Gough-Stewart platform consists of a moving platform connected to a fixed base via three linear actuators as shown in Figure 2.2. Changes in the actuator lengths result in changes in the position and orientation of the moving platform. This planar Gough-Stewart platform corresponds exactly to the simplified planar Stewart platform studied by Haug et al. [67].

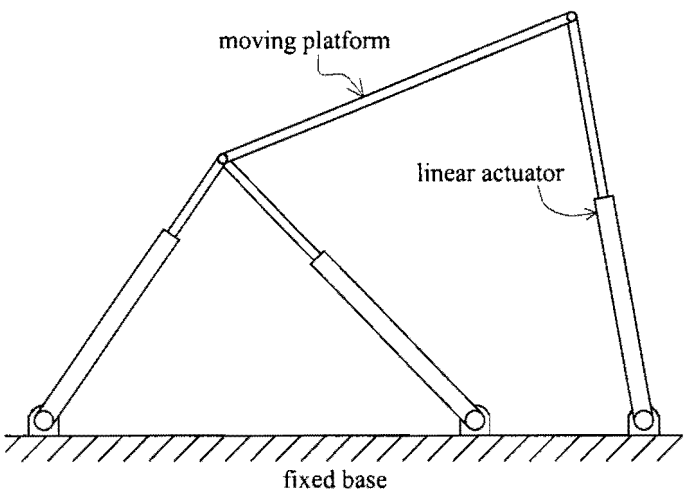

Figure 2.2: Planar Gough-Stewart platform.

A rigid body model is used for analysis purposes of the planar Gough-Stewart platform. Per definition a rigid body is a system of particles for which the distances between particles remain unchanged. Since all solid materials change shape to some extent when forces are applied to them, the concept of rigidity is only acceptable if the movement associated with the changes in shape is small compared with the overall movement of the body. In general this requirement is more than satisfied for most machining centers.

In order to specify the state of the planar Gough-Stewart platform, it is first necessary to define coordinates that specify the location and orientation of each body in the mechanism. Consider the illustrative example shown in Figure 2.3. The 0xy -coordinate system shown in Figure 2.3 is the global

reference frame, and a body-fixed $0_i\xi_i\eta_i$-coordinate system is embedded in body i. This implies that the position and orientation of body i can be specified in the plane by the position vector $\vec{\mathbf{r}}_i$, and the angle of rotation ϕ_i of the body-fixed $0_i\xi_i\eta_i$-coordinate system relative to the global coordinate system. The angle ϕ_i is considered positive if the rotation from positive x-axis to positive ξ_i-axis is counterclockwise (CCW).

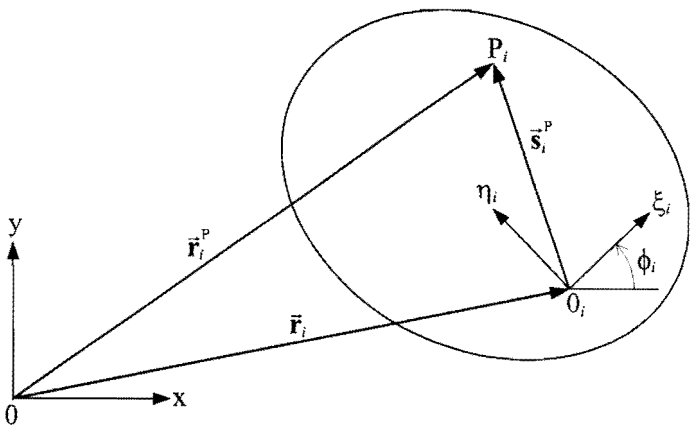

Figure 2.3: Locating point P relative to the body-fixed and global coordinate systems (after [65]).

A fixed point P_i on body i can be located from the origin of the $0_i\xi_i\eta_i$-axes by the vector $\vec{\mathbf{s}}_i^P$. The body-fixed point P_i can also be located from the origin of the global $0xy$-reference frame by vector $\vec{\mathbf{r}}_i^P$.

In general body i is not fixed, and therefore the physical vectors $\vec{\mathbf{r}}_i$, $\vec{\mathbf{r}}_i^P$ and $\vec{\mathbf{s}}_i^P$ are time varying vectors. Hence, the vector representations $\mathbf{r}_i$ and $\mathbf{r}_i^P$ of vectors $\vec{\mathbf{r}}_i$ and $\vec{\mathbf{r}}_i^P$ have components that vary with time t when represented in the global $0xy$-reference frame, i.e.

$$\vec{\mathbf{r}}_i : \mathbf{r}_i = \begin{bmatrix} x(t) \\ y(t) \end{bmatrix}_i \text{ and } \vec{\mathbf{r}}_i^P : \mathbf{r}_i^P = \begin{bmatrix} x^P(t) \\ y^P(t) \end{bmatrix}_i$$

Vector $\vec{\mathbf{s}}_i^P$ has *fixed* components when represented in the local $0_i\xi_i\eta_i$-reference frame, since point P_i is fixed in body i:

$$\vec{\mathbf{s}}_i^P : \mathbf{s}_i'^P = \begin{bmatrix} \xi^P \\ \eta^P \end{bmatrix}_i$$

The superscript prime $'$ indicates that the relevant vector is represented in the local coordinate system. It follows that vector $\vec{\mathbf{s}}_i^P$ represented in the global $0xy$-reference frame has time varying components indicated by $\mathbf{s}_i^P$. Figure 2.4 shows the geometrical relationship that exists between the global representation $\mathbf{s}_i^P$, and the local representation $\mathbf{s}_i'^P$ of vector $\vec{\mathbf{s}}_i^P$.

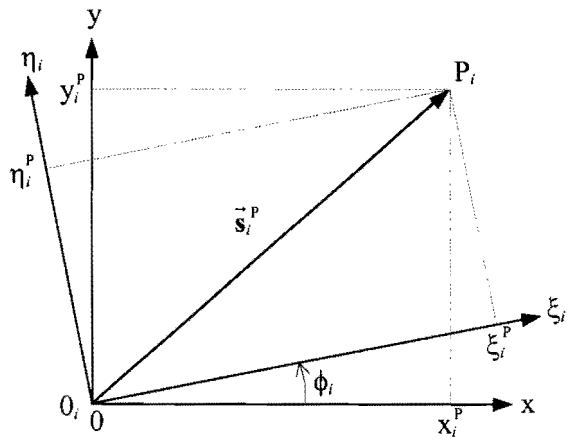

Figure 2.4: Translation between the local and global vector representations.

It follows directly from Figure 2.4 that

$$\mathbf{s}_i^P = \begin{bmatrix} x^P \\ y^P \end{bmatrix}_i = \begin{bmatrix} \xi_i^P \cos\phi_i - \eta_i^P \sin\phi_i \\ \xi_i^P \sin\phi_i + \eta_i^P \cos\phi_i \end{bmatrix} = \begin{bmatrix} \cos\phi_i & -\sin\phi_i \\ \sin\phi_i & \cos\phi_i \end{bmatrix} \begin{bmatrix} \xi^P \\ \eta^P \end{bmatrix}_i \tag{2.1}$$

or more concisely

$$\mathbf{s}_i^P = \mathbf{A}_i \mathbf{s}_i'^P \text{ with } \mathbf{A}_i = \begin{bmatrix} \cos\phi_i & -\sin\phi_i \\ \sin\phi_i & \cos\phi_i \end{bmatrix}$$

Furthermore, with reference to Figure 2.3:

$$\mathbf{r}_i^P = \mathbf{r}_i + \mathbf{s}_i^P = \mathbf{r}_i + \mathbf{A}_i \mathbf{s}_i'^P$$

In summary, it is noted that the position and orientation of body i may be represented in the x-y plane by the three-vector representation $\mathbf{q}_i$ consisting of the global components of vector $\mathbf{r}_i$ and the orientation angle ϕ_i, i.e.

$$\mathbf{q}_i = [\mathbf{r}^T, \phi]_i^T = [x, y, \phi]_i^T \tag{2.2}$$

The three components of $\mathbf{q}_i$ are called the *planar coordinates* of body *i*. It follows that for a system of b bodies situated in the x-y plane, the vector of coordinates for the b bodies is a 3b-vector given by

$$\mathbf{q} = [\mathbf{q}_1^T, \mathbf{q}_2^T, ..., \mathbf{q}_b^T]^T \tag{2.3}$$

Since the planar Gough-Stewart platform consists of eight bodies (see Figure 2.5), the coordinate vector of the entire mechanical system is a 24-vector, i.e.

$$\mathbf{q} = [\mathbf{q}_1^T, \mathbf{q}_2^T, ..., \mathbf{q}_8^T]^T = [x_1, y_1, \phi_1, x_2, y_2, \phi_2, ..., x_8, y_8, \phi_8]^T \tag{2.4}$$

where corresponding to Nikravesh [65], $\mathbf{q}$ without a subscript denotes the vector of coordinates for the entire system.

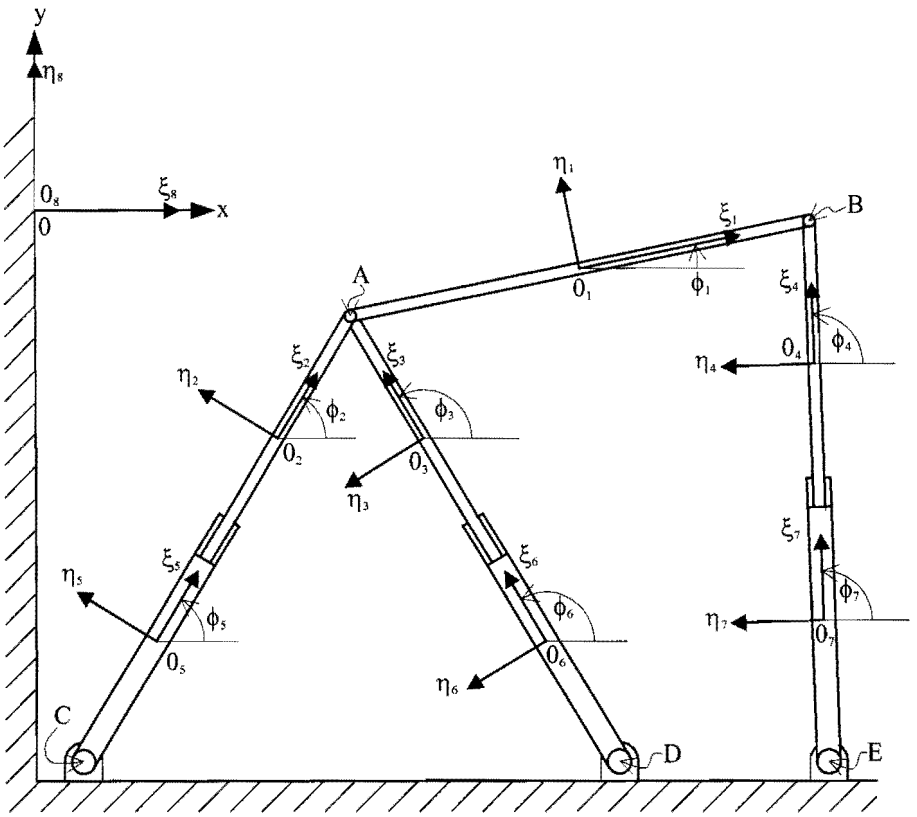

Figure 2.5: Planar Gough-Stewart platform, schematically represented as a mechanical system of eight bodies.

2.3 Kinematic constraint equations

In accordance with the definition of Nikravesh [65], the eight individual bodies that collectively form the planar Gough-Stewart platform shown in Figure 2.5, are called *links*. The combination of two links in contact constitutes a *kinematic pair*, or *joint*. An assemblage of interconnected links is called a *kinematic chain*. A mechanism is formed when at least one of the links of the kinematic chain is held fixed and any of its other links can move. The fixed link of the planar Gough-Stewart platform (link 8 in Figure 2.5) is the *ground* or *frame*. Note that the origin of link 8 is chosen to coincide with the origin of the global $0xy$-reference frame, and that the local $0_8\xi_8\eta_8$-coordinate system, and the global $0xy$-reference frame are identically orientated. Furthermore, the origin of each local $0_i\xi_i\eta_i$-coordinate system, $i = 1,2,...,7$, is chosen to coincide with the center of mass of respective bodies $1,2,...,7$, and these local coordinate systems are orientated as shown in Figure 2.5.

The primary purpose of the above schematic representation of the planar Gough-Stewart platform is to identify the *connectivity* of the bodies or links, i.e. to identify the *kinematic pairs* or *joints*. A kinematic pair imposes certain conditions on the relative motion between the two bodies it comprises. When these conditions are expressed in analytical form, they are called *equations of constraint*. Constraint equations

are denoted by Φ with a superscript indicating the constraint type and the number of algebraic equations, and a subscript indicating the joined bodies. Thus $\Phi_{i-j}^{(r,2)}$ denotes the revolute (r) joint constraint of joined bodies *i* and j, which consists of two equations. Similarly $\Phi_{i-j}^{(t,2)}$ denotes the translational joint (t) constraint of joined bodies *i* and j, which also contains two equations.

2.3.1 Revolute joints

With reference to Figure 2.5, the connections between the moving platform (link 1) and the upper portions of the actuator legs (links 2, 3 and 4) are revolute joints. This is also the case for the connections between ground (link 8) and the lower portions of the actuator legs (links 5, 6 and 7).

In order to find the two algebraic equations of $\Phi_{i-j}^{(r,2)}$, consider the schematic representation of a revolute joint connecting bodies *i* and j as shown in Figure 2.6. Point P denotes the center of the joint and can be considered to be two coincident points; i.e. point P_i on body *i* and point P_j on body j.

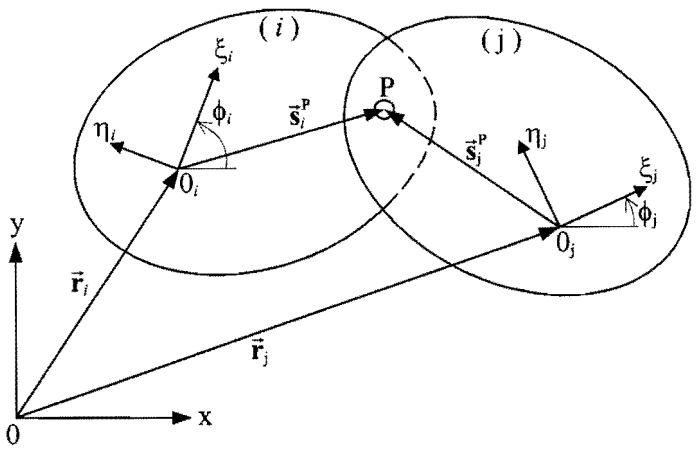

Figure 2.6: Revolute joint P connecting bodies *i* and j (after [65]).

The vectors $\vec{s}_i^P$ and $\vec{s}_j^P$ respectively describe the location of point P on body *i* and body j. Taken together with vectors $\vec{r}_i$ and $\vec{r}_j$, the constraint equations for the revolute joint are obtained from the closed vector loop expression:

$$\vec{r}_i + \vec{s}_i^P - \vec{s}_j^P - \vec{r}_j = \vec{0}$$

or in terms of global positional two-vectors:

$$\mathbf{r}_i + \mathbf{s}_i^P - \mathbf{s}_j^P - \mathbf{r}_j = \mathbf{0}$$

which is equivalent to

$$\Phi_{i-j}^{(r,2)} \equiv \mathbf{r}_i + \mathbf{A}_i \mathbf{s}_i'^P - \mathbf{r}_j - \mathbf{A}_j \mathbf{s}_j'^P = \mathbf{0} \qquad (2.5)$$

Expression (2.5) consists of two algebraic equations, i.e.

$$\mathbf{\Phi}_{i-j}^{(r,2)} \equiv \begin{bmatrix} x_i + \xi_i^P \cos\phi_i - \eta_i^P \sin\phi_i - x_j - \xi_j^P \cos\phi_j + \eta_j^P \sin\phi_j \\ y_i + \xi_i^P \sin\phi_i + \eta_i^P \cos\phi_i - y_j - \xi_j^P \sin\phi_j - \eta_j^P \cos\phi_j \end{bmatrix} = \begin{bmatrix} 0 \\ 0 \end{bmatrix} \tag{2.6}$$

These two constraint equations reduce the number of degrees of freedom (DOF) of the system of bodies shown in Figure 2.6, by two. Consequently, if the two bodies of Figure 2.6 are not connected to any other bodies, then the system has four DOF.

In particular, the constraint equations of the six revolute joints of the planar Gough-Stewart platform shown in Figure 2.5 are:

$$\mathbf{\Phi}_{1-2}^{(r,2)} \equiv \begin{bmatrix} x_1 + \xi_1^A \cos\phi_1 - \eta_1^A \sin\phi_1 - x_2 - \xi_2^A \cos\phi_2 + \eta_2^A \sin\phi_2 \\ y_1 + \xi_1^A \sin\phi_1 + \eta_1^A \cos\phi_1 - y_2 - \xi_2^A \sin\phi_2 - \eta_2^A \cos\phi_2 \end{bmatrix} = \begin{bmatrix} 0 \\ 0 \end{bmatrix} \tag{2.7}$$

$$\mathbf{\Phi}_{1-3}^{(r,2)} \equiv \begin{bmatrix} x_1 + \xi_1^A \cos\phi_1 - \eta_1^A \sin\phi_1 - x_3 - \xi_3^A \cos\phi_3 + \eta_3^A \sin\phi_3 \\ y_1 + \xi_1^A \sin\phi_1 + \eta_1^A \cos\phi_1 - y_3 - \xi_3^A \sin\phi_3 - \eta_3^A \cos\phi_3 \end{bmatrix} = \begin{bmatrix} 0 \\ 0 \end{bmatrix} \tag{2.8}$$

$$\mathbf{\Phi}_{1-4}^{(r,2)} \equiv \begin{bmatrix} x_1 + \xi_1^B \cos\phi_1 - \eta_1^B \sin\phi_1 - x_4 - \xi_4^B \cos\phi_4 + \eta_4^B \sin\phi_4 \\ y_1 + \xi_1^B \sin\phi_1 + \eta_1^B \cos\phi_1 - y_4 - \xi_4^B \sin\phi_4 - \eta_4^B \cos\phi_4 \end{bmatrix} = \begin{bmatrix} 0 \\ 0 \end{bmatrix} \tag{2.9}$$

$$\mathbf{\Phi}_{5-8}^{(r,2)} \equiv \begin{bmatrix} x_5 + \xi_5^C \cos\phi_5 - \eta_5^C \sin\phi_5 - x^C \\ y_5 + \xi_5^C \sin\phi_5 + \eta_5^C \cos\phi_5 - y^C \end{bmatrix} = \begin{bmatrix} 0 \\ 0 \end{bmatrix} \tag{2.10}$$

$$\mathbf{\Phi}_{6-8}^{(r,2)} \equiv \begin{bmatrix} x_6 + \xi_6^D \cos\phi_6 - \eta_6^D \sin\phi_6 - x^D \\ y_6 + \xi_6^D \sin\phi_6 + \eta_6^D \cos\phi_6 - y^D \end{bmatrix} = \begin{bmatrix} 0 \\ 0 \end{bmatrix} \tag{2.11}$$

$$\mathbf{\Phi}_{7-8}^{(r,2)} \equiv \begin{bmatrix} x_7 + \xi_7^E \cos\phi_7 - \eta_7^E \sin\phi_7 - x^E \\ y_7 + \xi_7^E \sin\phi_7 + \eta_7^E \cos\phi_7 - y^E \end{bmatrix} = \begin{bmatrix} 0 \\ 0 \end{bmatrix} \tag{2.12}$$

The simplification in expressions (2.10), (2.11) and (2.12) follow from the particular choice of position and orientation of the chosen local $0_8\xi_8\eta_8$ -coordinate system.

2.3.2 *Translational joints*

The three actuator legs shown in Figure 2.2, each consists of two links that translate with respect to each other parallel to an axis known as the *line of translation*. In particular, and with reference to Figure 2.5, the *left* actuator leg is a translational joint between links 2 and 5, the *middle* actuator leg is a translational joint between links 3 and 6 and the *right* actuator leg is a translational joint between links 4 and 7.

Figure 2.7 shows a schematic representation of a translational joint between links *i* and j, from which the two algebraic equations of $\mathbf{\Phi}_{i-j}^{(t,2)}$ may be derived.

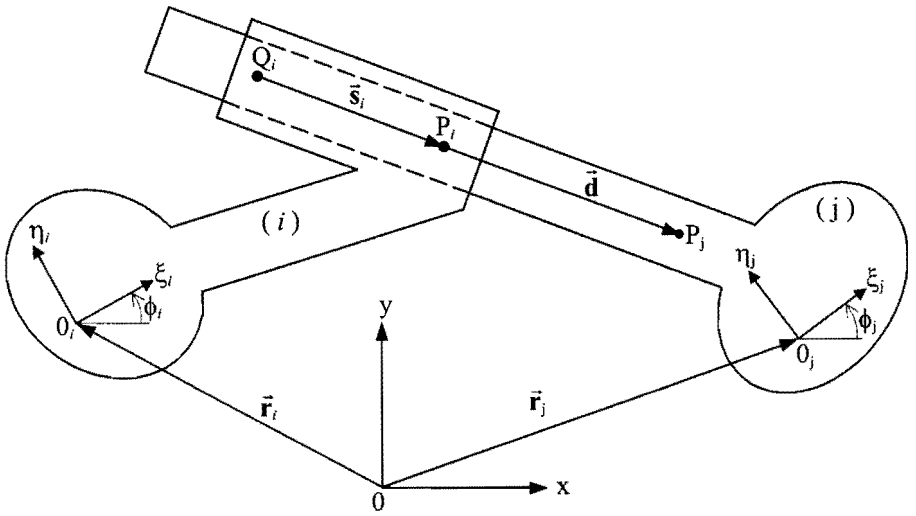

Figure 2.7: A translational joint between bodies *i* and j (after [65]).

A constraint is required to eliminate the relative motion between the two bodies in a direction perpendicular to the line of translation. In order to satisfy this constraint, the two vectors $\vec{\mathbf{s}}_i$ and $\vec{\mathbf{d}}$ shown in Figure 2.7 must remain parallel. These vectors are defined by locating three points on the line of translation – points Q_i and P_i on body *i*, and point P_j on body j. The first algebraic equation of $\mathbf{\Phi}_{i-j}^{(t,2)}$ follows from the fact that the vector product of two parallel vectors is zero, i.e.

$$\vec{\mathbf{s}}_i \times \vec{\mathbf{d}} = \vec{\mathbf{0}}$$

which, for the global components of vector $\vec{\mathbf{s}}_i$, i.e. $\vec{\mathbf{s}}_i : \mathbf{s}_i = \begin{bmatrix} (x_i^P - x_i^Q) \\ (y_i^P - y_i^Q) \end{bmatrix}$ and the global components of vector $\vec{\mathbf{d}}$, i.e. $\vec{\mathbf{d}} : \mathbf{d} = \begin{bmatrix} (x_j^P - x_i^P) \\ (y_j^P - y_i^P) \end{bmatrix}$, is equivalent to (see [65]):

$$(x_i^P - x_i^Q)(y_j^P - y_i^P) - (x_j^P - x_i^P)(y_i^P - y_i^Q) = 0 \qquad (2.13)$$

The second constraint of $\mathbf{\Phi}_{i-j}^{(t,2)}$ eliminates the relative rotation between bodies *i* and j, through the condition that

$$\phi_i - \phi_j - (\phi_i^0 - \phi_j^0) = 0 \qquad (2.14)$$

where ϕ_i^0 and ϕ_j^0 are the initial orientation angles.

The two constraint equations for a translational joint are therefore given by

$$\mathbf{\Phi}_{i-j}^{(t,2)} \equiv \begin{bmatrix} (x_i^P - x_i^Q)(y_j^P - y_i^P) - (x_j^P - x_i^P)(y_i^P - y_i^Q) \\ \phi_i - \phi_j - (\phi_i^0 - \phi_j^0) \end{bmatrix} = \begin{bmatrix} 0 \\ 0 \end{bmatrix} \qquad (2.15)$$

As in the case of the revolute joint, the translational joint reduces the number of degrees of freedom of a system by two.

Expression (2.13) may be expanded to give

$$x_i^P y_j^P - x_i^Q y_j^P + x_i^Q y_i^P - x_j^P y_i^P + x_j^P y_i^Q - x_i^P y_i^Q = 0 \qquad (2.16)$$

with

$$x_i^P = x_i + \xi_i^P \cos\phi_i - \eta_i^P \sin\phi_i \qquad y_i^P = y_i + \xi_i^P \sin\phi_i + \eta_i^P \cos\phi_i$$

$$x_i^Q = x_i + \xi_i^Q \cos\phi_i - \eta_i^Q \sin\phi_i \qquad y_i^Q = y_i + \xi_i^Q \sin\phi_i + \eta_i^Q \cos\phi_i$$

$$x_j^P = x_j + \xi_j^P \cos\phi_j - \eta_j^P \sin\phi_j \qquad y_j^P = y_j + \xi_j^P \sin\phi_j + \eta_j^P \cos\phi_j$$

Constraint (2.16) may therefore explicitly be stated in terms of the planar coordinates of two bodies.

With reference to Figure 2.5 the relevant vectors of translational joint $2-5$ are defined using points A and 0_2 in link 2, and point 0_5 in link 5. This implies that general constraint (2.16) corresponding to translational joint $2-5$, is:

$$x_2^{0_2} y_5^{0_5} - x_2^A y_5^{0_5} + x_2^A y_2^{0_2} - x_5^{0_5} y_2^{0_2} + x_5^{0_5} y_2^A - x_2^{0_2} y_2^A = 0$$

with

$$x_2^{0_2} = x_2 \qquad y_2^{0_2} = y_2$$

$$x_2^A = x_2 + \xi_2^A \cos\phi_2 \qquad y_2^A = y_2 + \xi_2^A \sin\phi_2$$

$$x_5^{0_5} = x_5 \qquad y_5^{0_5} = y_5$$

By substitution and simplification, the two constraint equations of the translational joint $2-5$ of the planar Gough-Stewart platform shown in Figure 2.5 are:

$$\mathbf{\Phi}_{2-5}^{(t,2)} \equiv \begin{bmatrix} -x_2\xi_2^A \sin\phi_2 + y_2\xi_2^A \cos\phi_2 + x_5\xi_2^A \sin\phi_2 - y_2\xi_2^A \cos\phi_2 \\ \phi_2 - \phi_5 \end{bmatrix} = \begin{bmatrix} 0 \\ 0 \end{bmatrix} \qquad (2.17)$$

Note that since the ξ_2 and ξ_5 axes coincide with the line of translation of translational joint $2-5$, the initial rotational angles ϕ_2^0 and ϕ_5^0 (see expressions (2.14) and (2.15)) fall away from the second constraint equation of $\mathbf{\Phi}_{2-5}^{(t,2)}$.

Similarly the constraint equations of translational joints $3-6$ and $4-7$ are respectively found to be

$$\mathbf{\Phi}_{3-6}^{(t,2)} \equiv \begin{bmatrix} -x_3\xi_3^A \sin\phi_3 + y_3\xi_3^A \cos\phi_3 + x_6\xi_3^A \sin\phi_3 - y_6\xi_3^A \cos\phi_3 \\ \phi_3 - \phi_6 \end{bmatrix} = \begin{bmatrix} 0 \\ 0 \end{bmatrix} \qquad (2.18)$$

$$\mathbf{\Phi}_{4-7}^{(t,2)} \equiv \begin{bmatrix} -x_4\xi_4^B \sin\phi_4 + y_4\xi_4^B \cos\phi_4 + x_7\xi_4^B \sin\phi_4 - y_7\xi_4^B \cos\phi_4 \\ \phi_4 - \phi_7 \end{bmatrix} = \begin{bmatrix} 0 \\ 0 \end{bmatrix} \qquad (2.19)$$

2.3.3 Simplified constraints

The remaining constraints are related to the fixed ground-link, i.e. link 8 of the planar Gough-Stewart platform (see Figure 2.5). In order to constrain the translation of the origin and angular motion of a fixed rigid body, the following three equations may be used as the necessary simplified constraints [65]:

$$\Phi \equiv x_i - c_1 = 0 \tag{2.20}$$

$$\Phi \equiv y_i - c_2 = 0 \tag{2.21}$$

$$\Phi \equiv \phi_i - c_3 = 0 \tag{2.22}$$

where c_1, c_2 and c_3 are constant quantities.

Since the origin of the local $0_8\xi_8\eta_8$-coordinate system coincides with the origin of the global $0xy$-reference frame, and the two coordinate systems are identically orientated (see Figure 2.5), expressions (2.20), (2.21) and (2.22) for link 8 of the planar Gough-Stewart platform, reduces to:

$$\Phi \equiv x_8 = 0 \tag{2.23}$$

$$\Phi \equiv y_8 = 0 \tag{2.24}$$

$$\Phi \equiv \phi_8 = 0 \tag{2.25}$$

For the eight-link kinematic model of the planar Gough-Stewart platform, the 21 *independent* kinematic constraint equations given by expressions (2.7) - (2.12), (2.17) - (2.19) and (2.23) - (2.25) apply. For a system having m *independent kinematic constraint equations* and n *coordinates*, the number of *degrees of freedom* (DOF) is given by:

$$k = n - m \tag{2.26}$$

Hence, the eight-link model of the planar Gough-Stewart platform has 24 coordinates, and consequently $24 - 21 = 3$ DOF.

2.4 Driving constraints

Any set of k coordinates that are *independent* and are equal in number to the number of DOF of the system, determines the values of the remaining m *dependent* coordinates through the solution of the m independent kinematic constraint equations. Thus for the planar Gough-Stewart platform with three DOF, the values of three *independent* coordinates must be known to completely describe the system.

In particular, the three planar coordinates describing the position and orientation of link 1, i.e. x_1, y_1 and ϕ_1 are the three independent coordinates of the planar Gough-Stewart platform shown in Figure 2.5.

The applicable *driving constraints* are equations expressing each independent coordinate as a function of time, i.e.:

$$\Phi^{(d-1,1)} \equiv x_1 - d_1(t) = 0 \tag{2.27}$$

$$\Phi^{(d-2,1)} \equiv y_1 - d_2(t) = 0 \tag{2.28}$$

$$\Phi^{(d-3,1)} \equiv \phi_1 - d_3(t) = 0 \tag{2.29}$$

Each driving constraint is denoted by Φ with the superscript indicating the driving constraint number, and the number of algebraic equations, e.g. $\Phi^{(d-1,1)}$ is driving constraint number 1, which involves 1 equation.

Expressions (2.27), (2.28) and (2.29) uniquely define the *motion* of link 1. With reference to Figure 2.2, link 1 is the moving platform of the planar Gough-Stewart platform and, with the planar machining center in mind, it is clear that in controlling the relative motion between the workpiece and cutting tool, either one can be attached to the moving platform with the other fixed in the plane.

These two possible scenarios are separately dealt with in the next two sub-sections, with specific reference to obtaining for a given tool path, expressions giving the required *values* of the three independent coordinates x_1, y_1 and ϕ_1 at any given time instant. The details of deriving the analytical functions $d_1(t)$, $d_2(t)$ and $d_3(t)$ that appear in driving constraints (2.27) - (2.29) are explained in **Chapter 3**.

2.4.1 Fixed workpiece

Consider the scenario of the cutting tool mounted on the moving platform with an externally *fixed workpiece* as shown in Figure 2.8. In this case it is required that the cutting tool be moved along a prescribed tool path specified in the global 0xy -coordinate system.

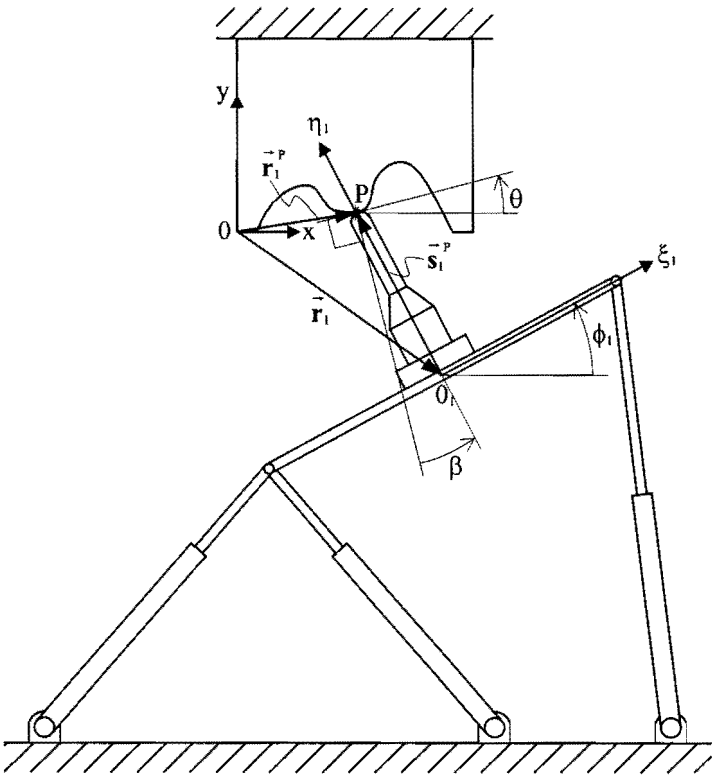

Figure 2.8: Fixed workpiece scenario.

At any given time instant it is assumed that the following are known:

1. the global position of the cutting tool tip (P in Figure 2.8) on the prescribed tool path, and
2. the angle β between the platform-mounted tool and the normal to the tool path at the point of contact (see Figure 2.8) and measured positive in the CCW direction.

Assumption 1 implies that the global representation of the time varying vector $\vec{r}_1^P$, i.e. $\vec{r}_1^P : \mathbf{r}_1^P = \begin{bmatrix} x^P \\ y^P \end{bmatrix}_1$ is known at every instant as the prescribed tool path is traced. The tool tip P can also be located relative to the origin of the local $0_1\xi_1\eta_1$-axes by the time varying vector $\vec{s}_1^P$. The corresponding fixed components of vector $\vec{s}_1^P$, when represented in the local $0_1\xi_1\eta_1$-reference frame, is $\vec{s}_1^P : \mathbf{s}_1'^P = \begin{bmatrix} 0 \\ \eta^P \end{bmatrix}_1$, where for any given tool length, the local η_1^P-component is a known constant.

The following vector loop equation may then be used to find the sought-after global position of link 1:

$$\vec{r}_1 + \vec{s}_1^P = \vec{r}_1^P$$

or in global vector representation:

$$\mathbf{r}_1 + \mathbf{A}_1\mathbf{s}_1'^P = \mathbf{r}_1^P$$

In terms of components this vector equation may be written as

$$\begin{bmatrix} x \\ y \end{bmatrix}_1 + \begin{bmatrix} \cos\phi_1 & -\sin\phi_1 \\ \sin\phi_1 & \cos\phi_1 \end{bmatrix} \begin{bmatrix} 0 \\ \eta^P \end{bmatrix}_1 = \begin{bmatrix} x^P \\ y^P \end{bmatrix}_1 \tag{2.30}$$

Expression (2.30) contains two scalar equations, i.e.

$$x_1 = x_1^P + \eta_1^P \sin\phi_1 \tag{2.31}$$

and

$$y_1 = y_1^P - \eta_1^P \cos\phi_1 \tag{2.32}$$

In order to compute x_1 and y_1, the orientation angle of link 1, ϕ_1, must also be known. At every time instant, as the cutting tool progresses along the prescribed tool path, the orientation angle ϕ_1 is directly related to the known prescribed angle β (see assumption 2 in Section 2.4.1). To find this relationship, consider the simplified fixed workpiece situation depicted in Figure 2.9, where the mounted cutting tool is collinear with the normal to the tool path at the point of contact.

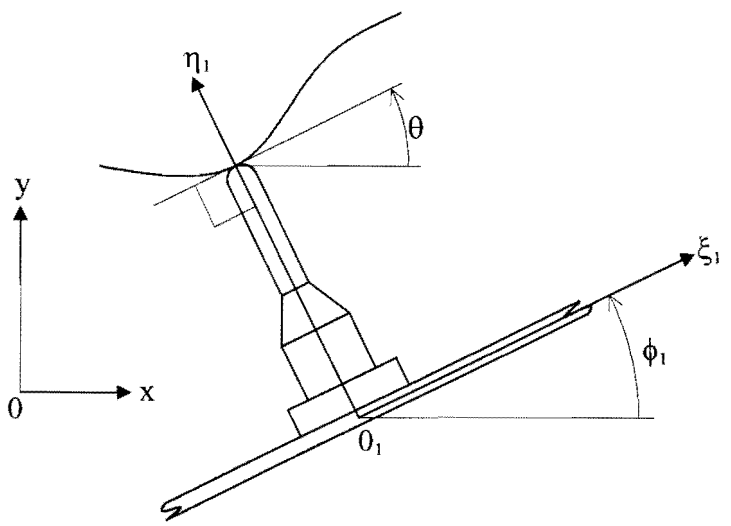

Figure 2.9: Simplified fixed workpiece situation.

For this situation, it is clear that $\beta = 0$ and the orientation angle ϕ_1 is equal to the gradient angle θ of the tool path, where

$$\tan\theta = \frac{dy}{dx} \tag{2.33}$$

and $\frac{dy}{dx}$ represents the (known) gradient of the prescribed tool path $y(x)$ at the point of contact.

With the proposed convention that β be measured positive CCW from the normal to the tool path at the point of contact, the orientation angle for the fixed workpiece situation depicted in Figure 2.8 is (remembering that for CW rotations θ and ϕ_1 take on negative values):

$$\phi_i = \theta + \beta \tag{2.34}$$

with ϕ_i and θ measured positive CCW from the horizontal, and β measured as defined above.

Substituting expression (2.34) into expressions (2.31) and (2.32) gives:

$$x_i = x_i^P + \eta_i^P \sin(\theta + \beta) \tag{2.35}$$

and

$$y_i = y_i^P - \eta_i^P \cos(\theta + \beta) \tag{2.36}$$

In summary, for the fixed tool scenario it follows that with x^P, y^P and β known at a specific time instant or point along the tool path, the corresponding independent coordinates of the planar Gough-Stewart platform, x_i, y_i and ϕ_i are respectively obtained by substituting the tool path gradient angle θ (see expression (2.33)) into expressions (2.35), (2.36) and (2.34).

2.4.2 *Fixed cutting tool*

The second planar machining center scenario is where the workpiece is mounted to the moving platform, and the cutting tool is externally fixed. This case is depicted in Figure 2.10, and since the tool path is now prescribed in terms of the local $0_i\xi_i\eta_i$-coordinate system, it is required that the workpiece be moved such that the fixed cutting tool traces the prescribed tool path.

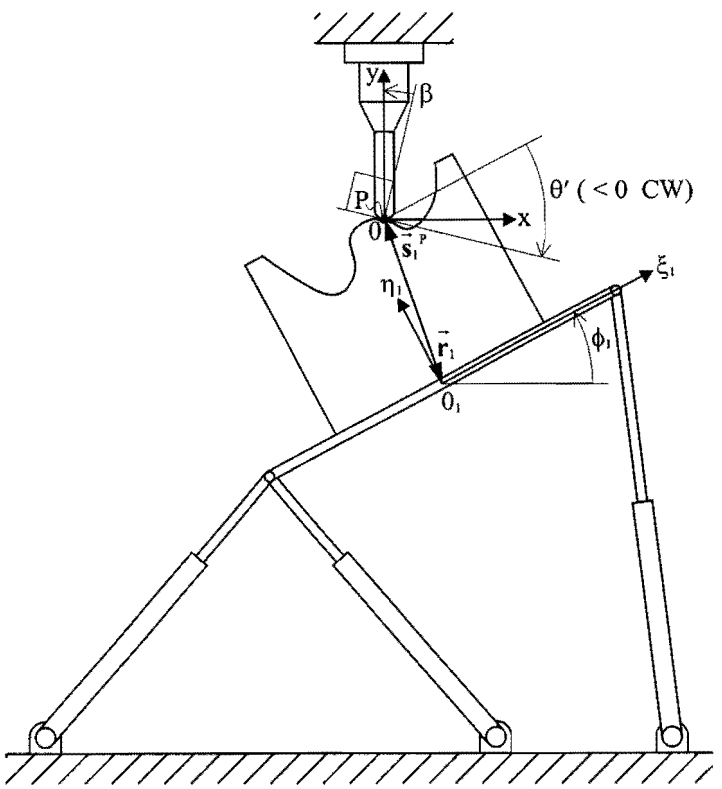

Figure 2.10: Fixed cutting tool scenario.

As in Section 2.4.1, it is also assumed here that at any time instant the following are known:

1. the local position of the cutting tool tip (P in Figure 2.10) on the prescribed tool path, and
2. the angle β (measured positive CCW), from the normal to the tool path at the point of contact, to the vertical axis of the fixed cutting tool (see Figure 2.10).

Assumption 1 implies that the local representation of the time varying vector $\vec{\mathbf{s}}_1^P$, i.e. $\vec{\mathbf{s}}_1^P : \mathbf{s}_1'^P = \begin{bmatrix} \xi^P \\ \eta^P \end{bmatrix}_1$ is known at every instant as the fixed cutting tool traces the prescribed tool path. The origin of the global reference frame is chosen to coincide with the tool tip P. Hence, vector $\vec{\mathbf{r}}_1$ locating the moving platform (link 1 in Figure 2.5) has the same magnitude as vector $\vec{\mathbf{s}}_1^P$, but is directed in the exact opposite direction.

To find the global components of vector $\vec{\mathbf{r}}_1$, first consider the simplified fixed cutting tool situation shown in Figure 2.11.

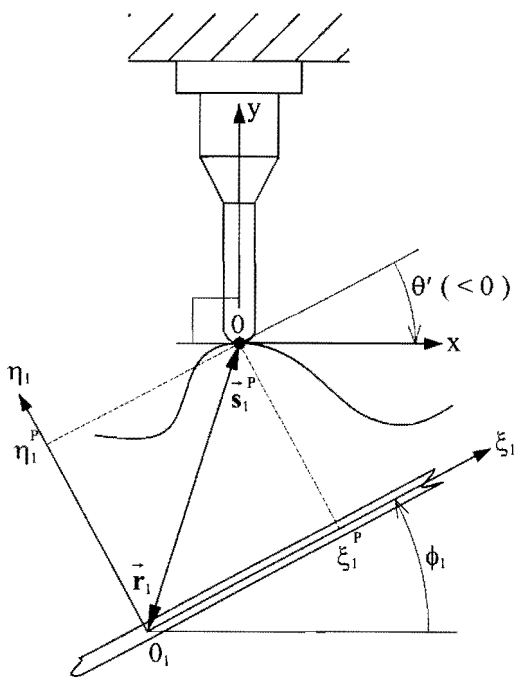

Figure 2.11: Simplified fixed cutting tool situation.

Clearly $\beta = 0$ in this case, which implies that the tangent to the prescribed tool path at the point of contact P is perpendicular to the vertical axis of the fixed cutting tool. The gradient angle of the prescribed tool path in the local coordinate system is θ', where

$$\tan\theta' = \frac{d\eta_1}{d\xi_1} \tag{2.37}$$

and $\frac{d\eta_1(\xi_1)}{d\xi_1}$ represents the gradient of the prescribed tool path $\eta_1(\xi_1)$ at the point of contact.

The superscript prime indicates that the gradient angle is determined relative to the local $0_1\xi_1\eta_1$-coordinate system.

For the simplified situation shown in Figure 2.11, the orientation angle ϕ_1 is equal in magnitude but oppositely orientated to the gradient angle θ', i.e. $\phi_1 = -\theta'$.

With ϕ_1 known, the global components of vector $\vec{r}_1$ are obtained using a translation that is similar to the one given by expression (2.1). In particular, the global components of vector $\vec{r}_1$ shown in Figure 2.11 are given by the following two scalar equations:

$$x_1 = -\xi_1^P \cos\phi_1 + \eta_1^P \sin\phi_1 \tag{2.38}$$

and

$$y_1 = -\xi_1^P \sin\phi_1 - \eta_1^P \cos\phi_1 \tag{2.39}$$

However, for the non-zero angle β shown in Figure 2.10, the orientation angle ϕ_1 of the moving platform is:

$$\phi_1 = -\theta' - \beta \tag{2.40}$$

using the CCW sign convention previously defined for all three angles.

Substituting expression (2.40) respectively into expressions (2.38) and (2.39) gives:

$$x_1 = -\xi_1^P \cos(\theta' + \beta) - \eta_1^P \sin(\theta' + \beta) \tag{2.41}$$

and

$$y_1 = \xi_1^P \sin(\theta' + \beta) - \eta_1^P \cos(\theta' + \beta) \tag{2.42}$$

Consequently, for the fixed cutting tool scenario with ξ_1^P, η_1^P and β known at any specific time instant, the corresponding independent coordinates of the planar Gough-Stewart platform x_1, y_1 and ϕ_1 are respectively obtained by substituting the tool path gradient angle θ' (see expression (2.37)) into expressions (2.41), (2.42) and (2.40).

2.5 Inverse kinematic analysis

In the kinematic analysis of the planar Gough-Stewart platform, the kinematic constraint equations derived in Section 2.3, and the driving constraints derived in Section 2.4 are used. The first and second time derivatives of these constraint equations yield the velocity and acceleration equations.

The method of appended driving constraints [65], is used here for the kinematic analysis of the planar Gough-Stewart platform. This method is presented below in its most general form.

Suppose that the vector of coordinates describing the configuration of a system is given by $\mathbf{q} = [q_1, q_2, ..., q_n]^T$ where n is the total number of coordinates. If there are m kinematic constraints expressed in vector form by $\mathbf{\Phi}(\mathbf{q}) = \mathbf{0}$, then k driving constraints can be appended to the kinematic constraints to obtain $n = m + k$ equations:

$$\mathbf{\Phi} \equiv \mathbf{\Phi}(\mathbf{q}) = \mathbf{0} \tag{2.43}$$

$$\mathbf{\Phi}^{(d)} \equiv \mathbf{\Phi}(\mathbf{q}, t) = \mathbf{0} \tag{2.44}$$

where the superscript (d) denotes the driving constraints. Expressions (2.43) and (2.44) represents n equations in n unknowns $\mathbf{q}$ which can be solved for any specific time t.

The velocity equations are obtained by taking the time derivative of expressions (2.43) and (2.44):

$$\mathbf{\Phi}_q \dot{\mathbf{q}} = \mathbf{0} \tag{2.45}$$

$$\mathbf{\Phi}_q^{(d)} \dot{\mathbf{q}} + \mathbf{\Phi}_t^{(d)} = \mathbf{0} \tag{2.46}$$

where $\mathbf{\Phi}_q$ represents the Jacobian of the vector function $\mathbf{\Phi}$ with respect to $\mathbf{q}$ and $\mathbf{\Phi}_t$ the partial derivative of the function with respect to t.

Expression (2.45) follows from the fact that in general:

$$\mathbf{\Phi}(\mathbf{q}) = \begin{bmatrix} \Phi_1(\mathbf{q}) \\ \Phi_2(\mathbf{q}) \\ \vdots \\ \Phi_m(\mathbf{q}) \end{bmatrix} \tag{2.47}$$

and therefore the time derivative of the *i*-th entry $\Phi_i(\mathbf{q})$ in expression (2.47) is:

$$\frac{d}{dt}\left(\Phi_i(\mathbf{q})\right) = \frac{\partial \Phi_i}{\partial q_1}\dot{q}_1 + \frac{\partial \Phi_i}{\partial q_2}\dot{q}_2 + \cdots + \frac{\partial \Phi_i}{\partial q_n}\dot{q}_n \tag{2.48}$$

Similarly, expression (2.46) follows from the fact that in general the driving constraints are also explicit functions of time:

$$\boldsymbol{\Phi}^{(d)}(\mathbf{q},t)=\begin{bmatrix}\Phi_1^{(d)}(\mathbf{q},t)\\ \Phi_2^{(d)}(\mathbf{q},t)\\ \vdots\\ \Phi_m^{(d)}(\mathbf{q},t)\end{bmatrix} \tag{2.49}$$

and therefore the corresponding time derivative of the i-th entry $\Phi_i^{(d)}(\mathbf{q},t)$ in expression (2.49) is given by

$$\frac{d}{dt}\left(\Phi_i^{(d)}(\mathbf{q},t)\right)=\frac{\partial\Phi_i^{(d)}}{\partial q_1}\dot{q}_1+\frac{\partial\Phi_i^{(d)}}{\partial q_2}\dot{q}_2+\cdots+\frac{\partial\Phi_i^{(d)}}{\partial q_n}\dot{q}_n+\frac{\partial\Phi_i^{(d)}}{\partial t} \tag{2.50}$$

The velocity equations (2.45) and (2.46) may also be written as

$$\begin{bmatrix}\boldsymbol{\Phi}_q\\ \boldsymbol{\Phi}_q^{(d)}\end{bmatrix}\dot{\mathbf{q}}=\begin{bmatrix}\mathbf{0}\\ -\boldsymbol{\Phi}_t^{(d)}\end{bmatrix} \tag{2.51}$$

which represents n algebraic equations, linear in terms of $\dot{\mathbf{q}}$.

The time derivative of expressions (2.45) and (2.46) yields the acceleration equations:

$$\boldsymbol{\Phi}_q\ddot{\mathbf{q}}+(\boldsymbol{\Phi}_q\dot{\mathbf{q}})_q\dot{\mathbf{q}}=\mathbf{0} \tag{2.52}$$

$$\boldsymbol{\Phi}_q^{(d)}\ddot{\mathbf{q}}+(\boldsymbol{\Phi}_q^{(d)}\dot{\mathbf{q}})_q\dot{\mathbf{q}}+2\boldsymbol{\Phi}_{qt}^{(d)}\dot{\mathbf{q}}+\boldsymbol{\Phi}_{tt}^{(d)}=\mathbf{0} \tag{2.53}$$

These expressions are obtained through the following argument. Considering the more general expression (2.46), which also contains t explicitly, it is clear that the left hand side is a vector function $\mathbf{F}$ of $\mathbf{q}$, $\dot{\mathbf{q}}$ and t:

$$\mathbf{F}(\mathbf{q},\dot{\mathbf{q}},t)=\boldsymbol{\Phi}_q(\mathbf{q},t)\dot{\mathbf{q}}+\boldsymbol{\Phi}_t(t,\mathbf{q}) \tag{2.54}$$

where for convenience the superscript has been dropped. The time derivative of (2.54) may therefore be written as

$$\frac{d\mathbf{F}}{dt}=\mathbf{F}_q\dot{\mathbf{q}}+\mathbf{F}_{\dot{q}}\ddot{\mathbf{q}}+\mathbf{F}_t \tag{2.55}$$

where $\mathbf{F}_q=[\boldsymbol{\Phi}_q\dot{\mathbf{q}}]_q+\boldsymbol{\Phi}_{tq}$,

$\mathbf{F}_{\dot{q}}=[\boldsymbol{\Phi}_q\dot{\mathbf{q}}]_{\dot{q}}+\boldsymbol{\Phi}_{t\dot{q}}=\boldsymbol{\Phi}_q$ and

$\mathbf{F}_t=\boldsymbol{\Phi}_{qt}\dot{\mathbf{q}}+\boldsymbol{\Phi}_{tt}$.

Substituting the above into (2.55) and then in (2.46) gives

$$\frac{d\mathbf{F}}{dt}=[\boldsymbol{\Phi}_q\dot{\mathbf{q}}]_q\dot{\mathbf{q}}+\boldsymbol{\Phi}_{tq}\dot{\mathbf{q}}+\boldsymbol{\Phi}_q\ddot{\mathbf{q}}+\boldsymbol{\Phi}_{qt}\dot{\mathbf{q}}+\boldsymbol{\Phi}_{tt}=\mathbf{0}$$

from which (2.53) [and also (2.52)] follows directly.

Accelerations equations (2.52) and (2.53) may also be written as

$$\begin{bmatrix} \Phi_q \\ \Phi_q^{(d)} \end{bmatrix} \ddot{\mathbf{q}} = \begin{bmatrix} -(\Phi_q \dot{\mathbf{q}})_q \dot{\mathbf{q}} \\ -(\Phi_q^{(d)} \dot{\mathbf{q}})_q \dot{\mathbf{q}} - 2\Phi_{qt}^{(d)} \dot{\mathbf{q}} - \Phi_{tt}^{(d)} \end{bmatrix} \tag{2.56}$$

which represents n algebraic equations linear in terms of $\ddot{\mathbf{q}}$.

For the planar Gough-Stewart platform under consideration, expression (2.43) represents the 21 equations given by expressions (2.7) - (2.12), (2.17) - (2.19) and (2.23) - (2.25), and expression (2.44) represents the three driving constraints given by expressions (2.27) - (2.29). These 24 nonlinear equations in 24 unknowns $\mathbf{q} = [x_1, y_1, \phi_1, x_2, y_2, \phi_2, ..., x_8, y_8, \phi_8]^T$ (see expression (2.4)) may therefore be solved for any specified time t.

More specifically, at any specified time t, expressions (2.27) - (2.29) provide the x_1, y_1 and ϕ_1 values. With reference to Figure 2.5, the global coordinates of points A and B are

$$\begin{aligned} x^A &= x_1 + \xi_1^A \cos\phi_1 & y^A &= y_1 + \xi_1^A \sin\phi_1 \\ x^B &= x_1 + \xi_1^B \cos\phi_1 & y^B &= y_1 + \xi_1^B \sin\phi_1 \end{aligned} \tag{2.57}$$

Note that for the specific choice of the local coordinate system of body 1 coinciding with the center of mass of body 1 (see Section 2.3), $\xi_1^A < 0$.

The global positions of points C, D and E are also known for any specific design of the planar Gough-Stewart platform.

The orientation angles of links 2 - 7 may be determined using the "two-argument arc tangent function" $\text{a tan 2}\left(\frac{y}{x}\right)$. In particular, $\text{a tan 2}\left(\frac{y}{x}\right)$ denotes the angle whose tangent is y divided by x. Moreover, both the magnitudes and signs of x and y are used in the definition, so that angles are uniquely defined in all four quadrants. For example: $\text{a tan 2}\left(\frac{-1.0}{-1.0}\right) = -135°$, and $\text{a tan 2}\left(\frac{1.0}{1.0}\right) = 45°$ (see [60]).

For the specific choice of local axes shown in Figure 2.5, the respective orientation angles of links 2 and 5, links 3 and 6 as well as links 4 and 7 are equal, i.e.

$$\phi_2 = \phi_5 = a\tan 2\left(\frac{y^A - y^C}{x^A - x^C}\right) \tag{2.58}$$

$$\phi_3 = \phi_6 = a\tan 2\left(\frac{y^A - y^D}{x^A - x^D}\right) \tag{2.59}$$

$$\phi_4 = \phi_7 = a\tan 2\left(\frac{y^B - y^E}{x^B - x^E}\right) \tag{2.60}$$

Note that the revolute joint constraints given by expressions (2.7) - (2.12), as well as the translational joint constraints given by expressions (2.17) - (2.19) are implicitly satisfied in expressions (2.58) - (2.60).

The global positions of links 2 – 7 follow directly from the transformation given by expression (2.1), i.e.

$$\begin{aligned}
x_2 &= x^A - \xi_2^A \cos\phi_2 & y_2 &= y^A - \xi_2^A \sin\phi_2 \\
x_3 &= x^A - \xi_3^A \cos\phi_3 & y_3 &= y^A - \xi_3^A \sin\phi_3 \\
x_4 &= x^B - \xi_4^B \cos\phi_4 & y_4 &= y^B - \xi_4^B \sin\phi_4 \\
x_5 &= x^C - \xi_5^C \cos\phi_5 & y_5 &= y^C - \xi_5^C \sin\phi_5 \\
x_6 &= x^D - \xi_6^D \cos\phi_6 & y_6 &= y^D - \xi_6^D \sin\phi_6 \\
x_7 &= x^E - \xi_7^E \cos\phi_7 & y_7 &= y^E - \xi_7^E \sin\phi_7
\end{aligned} \tag{2.61}$$

The global positions and orientation of link 8 (ground) is given by expressions (2.23) - (2.25), i.e. $x_8 = 0$, $y_8 = 0$ and $\phi_8 = 0$. With a known coordinate vector $\mathbf{q} = [x_1, y_1, \phi_1, x_2, y_2, \phi_2, \ldots, x_8, y_8, \phi_8]^T$, the Jacobian matrix $\mathbf{J} = \begin{bmatrix} \mathbf{\Phi}_\mathbf{q} \\ \mathbf{\Phi}_\mathbf{q}^{(d)} \end{bmatrix}$ of the planar Gough-Stewart platform is uniquely defined (see following expression (2.62)):

$$
\mathbf{J} = \begin{bmatrix}
1 & 0 & -\xi_1^A \sin\phi_1 & -1 & 0 & \xi_2^A \sin\phi_2 & 0 & 0 & 0 & 0 & 0 & 0 & 0 & 0 & 0 & 0 & 0 & 0 & 0 & 0 & 0 & 0 & 0 & 0 \\
0 & 1 & \xi_1^A \cos\phi_1 & 0 & -1 & -\xi_2^A \cos\phi_2 & 0 & 0 & 0 & 0 & 0 & 0 & 0 & 0 & 0 & 0 & 0 & 0 & 0 & 0 & 0 & 0 & 0 & 0 & 0 \\
1 & 0 & -\xi_1^A \sin\phi_1 & 0 & 0 & 0 & -1 & 0 & \xi_3^A \sin\phi_3 & 0 & 0 & 0 & 0 & 0 & 0 & 0 & 0 & 0 & 0 & 0 & 0 & 0 & 0 & 0 & 0 \\
0 & 1 & \xi_1^A \cos\phi_1 & 0 & 0 & 0 & 0 & -1 & -\xi_3^A \cos\phi_3 & 0 & 0 & 0 & 0 & 0 & 0 & 0 & 0 & 0 & 0 & 0 & 0 & 0 & 0 & 0 & 0 \\
1 & 0 & -\xi_1^B \sin\phi_1 & 0 & 0 & 0 & 0 & 0 & 0 & -1 & 0 & \xi_4^B \sin\phi_4 & 0 & 0 & 0 & 0 & 0 & 0 & 0 & 0 & 0 & 0 & 0 & 0 & 0 \\
0 & 1 & \xi_1^B \cos\phi_1 & 0 & 0 & 0 & 0 & 0 & 0 & 0 & -1 & -\xi_4^B \cos\phi_4 & 0 & 0 & 0 & 0 & 0 & 0 & 0 & 0 & 0 & 0 & 0 & 0 & 0 \\
0 & 0 & 0 & 0 & 0 & 0 & 0 & 0 & 0 & 0 & 0 & 0 & 1 & 0 & -\xi_5^C \sin\phi_5 & 0 & 0 & 0 & 0 & 0 & 0 & 0 & 0 & 0 & 0 \\
0 & 0 & 0 & 0 & 0 & 0 & 0 & 0 & 0 & 0 & 0 & 0 & 0 & 1 & \xi_5^C \cos\phi_5 & 0 & 0 & 0 & 0 & 0 & 0 & 0 & 0 & 0 & 0 \\
0 & 0 & 0 & 0 & 0 & 0 & 0 & 0 & 0 & 0 & 0 & 0 & 0 & 0 & 0 & 1 & 0 & -\xi_6^D \sin\phi_6 & 0 & 0 & 0 & 0 & 0 & 0 & 0 \\
0 & 0 & 0 & 0 & 0 & 0 & 0 & 0 & 0 & 0 & 0 & 0 & 0 & 0 & 0 & 0 & 1 & \xi_6^D \cos\phi_6 & 0 & 0 & 0 & 0 & 0 & 0 & 0 \\
0 & 0 & 0 & 0 & 0 & 0 & 0 & 0 & 0 & 0 & 0 & 0 & 0 & 0 & 0 & 0 & 0 & 0 & 1 & 0 & -\xi_7^E \sin\phi_7 & 0 & 0 & 0 & 0 \\
0 & 0 & 0 & 0 & 0 & 0 & 0 & 0 & 0 & 0 & 0 & 0 & 0 & 0 & 0 & 0 & 0 & 0 & 0 & 1 & \xi_7^E \cos\phi_7 & 0 & 0 & 0 & 0 \\
0 & 0 & 0 & -\xi_2^A \sin\phi_2 & \xi_2^A \cos\phi_2 & \begin{matrix} -x_2\xi_2^A \cos\phi_2 \\ -y_2\xi_2^A \sin\phi_2 \\ +x_3\xi_2^A \cos\phi_2 \\ +y_3\xi_2^A \sin\phi_2 \end{matrix} & 0 & 0 & 0 & 0 & 0 & 0 & \xi_2^A \sin\phi_2 & -\xi_2^A \cos\phi_2 & 0 & 0 & 0 & 0 & 0 & 0 & 0 & 0 & 0 & 0 & 0 \\
0 & 0 & 0 & 0 & 0 & -1 & 0 & 0 & \begin{matrix} 0 \\ -x_3\xi_3^A \cos\phi_3 \\ -y_3\xi_3^A \sin\phi_3 \\ +x_6\xi_3^A \cos\phi_1 \\ +y_6\xi_3^A \sin\phi_3 \end{matrix} & 0 & 0 & 0 & 0 & 0 & 1 & 0 & 0 & 0 & 0 & 0 & 0 & 0 & 0 & 0 & 0 & 0 \\
0 & 0 & 0 & 0 & 0 & 0 & -\xi_3^A \sin\phi_1 & \xi_3^A \cos\phi_3 & 0 & 0 & 0 & 0 & 0 & 0 & 0 & \xi_3^A \sin\phi_3 & -\xi_3^A \cos\phi_3 & 0 & 0 & 0 & 0 & 0 & 0 & 0 & 0 \\
0 & 0 & 0 & 0 & 0 & 0 & 0 & 0 & \begin{matrix} -1 \\ -x_4\xi_4^B \cos\phi_4 \end{matrix} & 0 & 0 & 0 & 0 & 0 & 0 & 0 & 0 & 1 & 0 & 0 & 0 & 0 & 0 & 0 & 0 \\
0 & 0 & 0 & 0 & 0 & 0 & 0 & 0 & 0 & -\xi_4^B \sin\phi_4 & \xi_4^B \cos\phi_4 & \begin{matrix} -y_4\xi_4^B \sin\phi_4 \\ +x_7\xi_4^B \cos\phi_4 \\ +y_7\xi_4^B \sin\phi_4 \end{matrix} & 0 & 0 & 0 & 0 & 0 & 0 & 0 & \xi_4^B \sin\phi_4 & -\xi_4^B \cos\phi_4 & 0 & 0 & 0 & 0 \\
0 & 0 & 0 & 0 & 0 & 0 & 0 & 0 & 0 & 0 & 0 & -1 & 0 & 0 & 0 & 0 & 0 & 0 & 0 & 0 & 1 & 0 & 0 & 0 & 0 \\
0 & 0 & 0 & 0 & 0 & 0 & 0 & 0 & 0 & 0 & 0 & 0 & 0 & 0 & 0 & 0 & 0 & 0 & 0 & 0 & 0 & 1 & 0 & 0 & 0 \\
0 & 0 & 0 & 0 & 0 & 0 & 0 & 0 & 0 & 0 & 0 & 0 & 0 & 0 & 0 & 0 & 0 & 0 & 0 & 0 & 0 & 0 & 1 & 0 & 0 \\
0 & 0 & 0 & 0 & 0 & 0 & 0 & 0 & 0 & 0 & 0 & 0 & 0 & 0 & 0 & 0 & 0 & 0 & 0 & 0 & 0 & 0 & 0 & 1 & 0 \\
0 & 0 & 0 & 0 & 0 & 0 & 0 & 0 & 0 & 0 & 0 & 0 & 0 & 0 & 0 & 0 & 0 & 0 & 0 & 0 & 0 & 0 & 0 & 0 & 1 \\
1 & 0 & 0 & 0 & 0 & 0 & 0 & 0 & 0 & 0 & 0 & 0 & 0 & 0 & 0 & 0 & 0 & 0 & 0 & 0 & 0 & 0 & 0 & 0 & 0 \\
0 & 1 & 0 & 0 & 0 & 0 & 0 & 0 & 0 & 0 & 0 & 0 & 0 & 0 & 0 & 0 & 0 & 0 & 0 & 0 & 0 & 0 & 0 & 0 & 0 \\
0 & 0 & 1 & 0 & 0 & 0 & 0 & 0 & 0 & 0 & 0 & 0 & 0 & 0 & 0 & 0 & 0 & 0 & 0 & 0 & 0 & 0 & 0 & 0 & 0
\end{bmatrix} \tag{2.62}
$$

The right hand side of expression (2.51) as applied to the planar Gough-Stewart platform is

$$\begin{bmatrix} \mathbf{0} \\ -\boldsymbol{\Phi}_t^{(d)} \end{bmatrix} = \begin{bmatrix} 0 \\ 0 \\ \vdots \\ 0 \\ \dfrac{\partial}{\partial t} d_1(t) \\ \dfrac{\partial}{\partial t} d_2(t) \\ \dfrac{\partial}{\partial t} d_3(t) \end{bmatrix} \tag{2.63}$$

The partial derivatives of the three driving constraints with respect to time are the velocities of link 1, i.e.: $\frac{\partial}{\partial t} d_1(t) = \dot{x}_1(t)$, $\frac{\partial}{\partial t} d_2(t) = \dot{y}_1(t)$ and $\frac{\partial}{\partial t} d_3(t) = \dot{\phi}_1(t)$, the calculation of which, for a specific tool path, is explained in **Chapter 3**.

Substituting expressions (2.62) and (2.63) into expression (2.51) results in 24 algebraic equations, linear in terms of $\dot{\mathbf{q}}$, where $\dot{\mathbf{q}} = [\dot{x}_1, \dot{y}_1, \dot{\phi}_1, \dot{x}_2, \dot{y}_2, \dot{\phi}_2, ..., \dot{x}_8, \dot{y}_8, \dot{\phi}_8]^T$ is the velocity vector of the planar Gough-Stewart platform. This linear system, of the general form $\mathbf{Ax} = \mathbf{c}$, is solved using the L-U factorization method. This method is a compact form of the Gaussian elimination method of operating on matrix **A**. After the operation is completed, the set of linear equations $\mathbf{Ax} = \mathbf{c}$ is efficiently solved for any given **c** vector (see [65] and [55]).

In the linear system (2.56), the Jacobian matrix (expression (2.62)) is also required to solve for the accelerations of the planar Gough-Stewart platform, i.e. for $\ddot{\mathbf{q}} = [\ddot{x}_1, \ddot{y}_1, \ddot{\phi}_1, \ddot{x}_2, \ddot{y}_2, \ddot{\phi}_2, ..., \ddot{x}_8, \ddot{y}_8, \ddot{\phi}_8]^T$. The right hand side of expression (2.56) is a 24 vector given by

$$\begin{bmatrix} -(\Phi_q \dot{q})_q \dot{q} \\ -(\Phi_q^{(d)} \dot{q})_q \dot{q} - 2\Phi_{qt}^{(d)} \dot{q} - \Phi_{tt}^{(d)} \end{bmatrix} = \begin{bmatrix} (\dot{\phi}_1)^2 \xi_1^A \cos\phi_1 - (\dot{\phi}_2)^2 \xi_2^A \cos\phi_2 \\ (\dot{\phi}_1)^2 \xi_1^A \sin\phi_1 - (\dot{\phi}_2)^2 \xi_2^A \sin\phi_2 \\ (\dot{\phi}_1)^2 \xi_1^A \cos\phi_1 - (\dot{\phi}_3)^2 \xi_3^A \cos\phi_3 \\ (\dot{\phi}_1)^2 \xi_1^A \sin\phi_1 - (\dot{\phi}_3)^2 \xi_3^A \sin\phi_3 \\ (\dot{\phi}_1)^2 \xi_1^B \cos\phi_1 - (\dot{\phi}_4)^2 \xi_4^B \cos\phi_4 \\ (\dot{\phi}_1)^2 \xi_1^B \sin\phi_1 - (\dot{\phi}_4)^2 \xi_4^B \sin\phi_4 \\ (\dot{\phi}_5)^2 \xi_5^C \cos\phi_5 \\ (\dot{\phi}_5)^2 \xi_5^C \sin\phi_5 \\ (\dot{\phi}_6)^2 \xi_6^D \cos\phi_6 \\ (\dot{\phi}_6)^2 \xi_6^D \sin\phi_6 \\ (\dot{\phi}_7)^2 \xi_7^E \cos\phi_7 \\ (\dot{\phi}_7)^2 \xi_7^E \sin\phi_7 \\ \left(2\dot{x}_2 - 2\dot{x}_5 + y_2\dot{\phi}_2 - y_5\dot{\phi}_5\right)\dot{\phi}_2 \xi_2^A \cos\phi_2 + \left(2\dot{y}_2 - 2\dot{y}_5 - x_2\dot{\phi}_2 + x_5\dot{\phi}_5\right)\dot{\phi}_2 \xi_2^A \sin\phi_2 \\ 0 \\ \left(2\dot{x}_3 - 2\dot{x}_6 + y_3\dot{\phi}_3 - y_6\dot{\phi}_6\right)\dot{\phi}_3 \xi_3^A \cos\phi_3 + \left(2\dot{y}_3 - 2\dot{y}_6 - x_3\dot{\phi}_3 + x_6\dot{\phi}_6\right)\dot{\phi}_3 \xi_3^A \sin\phi_3 \\ 0 \\ \left(2\dot{x}_4 - 2\dot{x}_7 + y_4\dot{\phi}_4 - y_7\dot{\phi}_4\right)\dot{\phi}_4 \xi_4^B \cos\phi_4 + \left(2\dot{y}_4 - 2\dot{y}_7 - x_4\dot{\phi}_4 + x_7\dot{\phi}_4\right)\dot{\phi}_4 \xi_4^B \sin\phi_4 \\ 0 \\ 0 \\ 0 \\ 0 \\ \frac{\partial^2}{\partial t^2} d_1(t) \\ \frac{\partial^2}{\partial t^2} d_2(t) \\ \frac{\partial^2}{\partial t^2} d_3(t) \end{bmatrix} \tag{2.64}$$

The second partial derivatives of the driving constraints with respect to time are the accelerations of link 1, i.e.: $\frac{\partial^2}{\partial t^2} d_1(t) = \ddot{x}_1(t)$, $\frac{\partial^2}{\partial t^2} d_2(t) = \ddot{y}_1(t)$ and $\frac{\partial^2}{\partial t^2} d_3(t) = \ddot{\phi}_1(t)$. Again the calculation of these accelerations for a prescribed tool path will be explained in **Chapter 3**.

Substituting expressions (2.62) and (2.64) into expression (2.56) results in 24 algebraic equations, linear in terms of $\ddot{\mathbf{q}}$, which can again be solved using the L-U factorization method.

2.6 Kinetic analysis

Kinetics is the study of motion and its relationship with the forces that produce the motion (see Figure 2.1). Using Newton's second law, the *equations of motion* of a continuous rigid body are derived in **Appendix A**. This Section deals with the application of the equations of motion to a general system of unconstrained bodies experiencing planar motion. The underlying theory is also applied to a system of constrained bodies experiencing planar motion with specific reference to the planar Gough-Stewart platform.

2.6.1 Planar equations of motion for a system of unconstrained bodies

The equations of motion for a single unconstrained body moving in the plane (see **Appendix A**) may be written in matrix form as

$$\begin{bmatrix} m & & \\ & m & \\ & & \mu \end{bmatrix}_i \begin{bmatrix} \ddot{x} \\ \ddot{y} \\ \ddot{\phi} \end{bmatrix}_i = \begin{bmatrix} f_{(x)} \\ f_{(y)} \\ n \end{bmatrix}_i \tag{2.65}$$

where for notational simplicity the polar moment of inertia j_{zz} is denoted by μ (see [65]). The subscript i in expression (2.65) indicates that these are the equations of motion of body i.

According to Nikravesh [65], expression (2.65) may also be written as

$$\mathbf{M}_i\ddot{\mathbf{q}}_i = \mathbf{g}_i \tag{2.66}$$

where $\mathbf{M}_i = \text{diag}[m, m, \mu]_i$,

$\mathbf{q}_i = [x, y, \phi]_i^T$ and

$\mathbf{g}_i = [f_{(x)}, f_{(y)}, n]_i^T$.

Furthermore, for a *system* of b *unconstrained* bodies, expression (2.66) is repeated b times to give

$$\mathbf{M}\ddot{\mathbf{q}} = \mathbf{g} \tag{2.67}$$

where $\mathbf{M} = \text{diag}[\mathbf{M}_1, \mathbf{M}_2, ..., \mathbf{M}_b]$,

$\mathbf{q} = [\mathbf{q}_1^T, \mathbf{q}_2^T, ..., \mathbf{q}_b^T]^T$ and

$\mathbf{g} = [\mathbf{g}_1^T, \mathbf{g}_2^T, ..., \mathbf{g}_b^T]^T$.

The system mass matrix $\mathbf{M}$ is a $n \times n$ constant diagonal matrix, and vectors $\mathbf{q}$, $\dot{\mathbf{q}}$, $\ddot{\mathbf{q}}$ and $\mathbf{g}$ are n vectors. Note that $n = 3b$, where n is the number of coordinates of the system of b bodies (see expression (2.3)).

2.6.2 Planar equations of motion for a system of constrained bodies.

If the system of bodies is interconnected by kinematic joints, it is referred to as a system of constrained bodies.

In general the system vector of coordinates for b constrained bodies is denoted by $\mathbf{q}$ (see expression (2.3)). Furthermore the kinematic joints in the system can be represented as m independent constraints $\mathbf{\Phi}(\mathbf{q}) = \mathbf{0}$ as given in expression (2.43). These m independent equations are normally nonlinear in terms of $\mathbf{q}$ (see expression (2.47)).

Each kinematic joint introduces reaction forces between connecting bodies. These reaction forces, which are also referred to as constraint forces, are denoted by vector $\mathbf{g}^{(c)}$:

$$\mathbf{g}^{(c)} = \left[\mathbf{g}_1^{(c)^T}, \mathbf{g}_2^{(c)^T}, \ldots, \mathbf{g}_b^{(c)^T}\right]^T \tag{2.68}$$

where $\mathbf{g}_i^{(c)}$, $i = 1,2,\ldots,b$ is the vector of the resultant of the joint reaction forces acting on body *i*. The sum of the constraint forces $\mathbf{g}^{(c)}$ and the external forces $\mathbf{g}$ provides the total forces acting on the system. Hence, expression (2.67) may be rewritten to read:

$$\mathbf{M}\ddot{\mathbf{q}} = \mathbf{g} + \mathbf{g}^{(c)} \tag{2.69}$$

For a system of constrained bodies experiencing planar motion, the reaction forces represented by expression (2.68) may be expressed in terms of the same coordinate system as the vector of coordinates $\mathbf{q}$.

Consider the planar example shown in Figure 2.12, where the reaction force $\vec{\mathbf{R}}$ is acting on the body *i* at the revolute joint P. The three coordinates of the body follow from expression (2.2), i.e., $\mathbf{q}_i = [\mathbf{r}^T, \phi]_i^T = [x, y, \phi]_i^T$ and the local coordinate system is assumed to be centered at C_i the center of mass of body *i* (see Section 2.3). For convenience the subscript *i* is dropped in what follows.

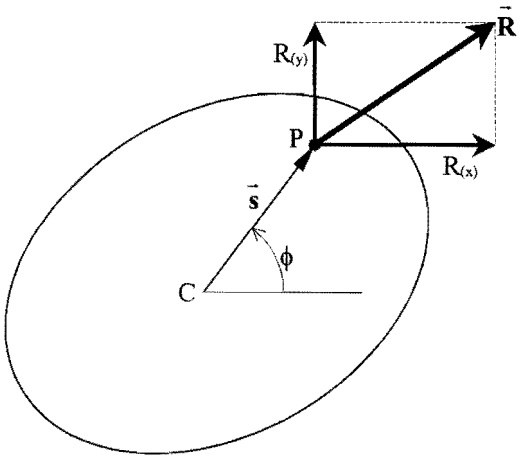

Figure 2.12: Planar body with reaction force applied at the revolute joint.

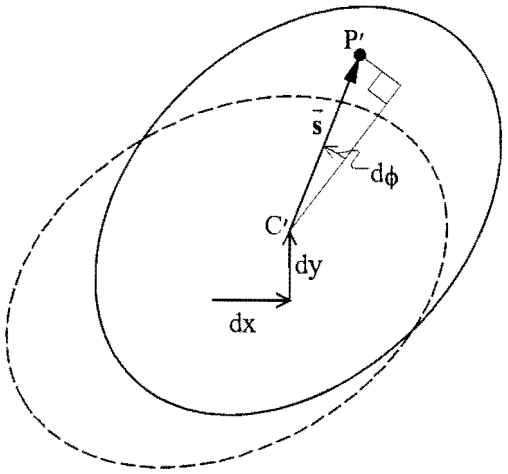

Figure 2.13: Virtual displacement of planar body.

If the body undergoes a virtual displacement such that C' is the new position of the center of mass, and P' is the new position of the revolute joint (see Figure 2.13), the corresponding work done by the reaction force $\vec{\mathbf{R}}$ is

$$\begin{aligned} dW &= R_{(x)}(dx - sd\phi \sin\phi) + R_{(y)}(dy + sd\phi \cos\phi) \\ &= R_{(x)}dx + R_{(y)}dy + (-R_{(x)}s\sin\phi + R_{(y)}s\cos\phi)d\phi \\ &= g_{(x)}dx + g_{(y)}dy + g_{(\phi)}d\phi \end{aligned}$$

Thus, the reaction force $\vec{\mathbf{R}}$ may be represented by a three-vector $\mathbf{g}$ with each component associated with a planar coordinate, i.e., $\mathbf{g} = [g_{(x)}, g_{(y)}, g_{(\phi)}]^T$. The three components of $\mathbf{g}$ are consistent with the three coordinates x, y and ϕ and are called the *generalized forces* associated with the chosen coordinates $\mathbf{q}$.

The introduction of generalized forces allows for the constraint force vector $\mathbf{g}^{(c)}$ to be expressed in terms of the constraint equations $\mathbf{\Phi}$ given by expression (2.43). In particular expression (2.43) contains m independent constraint equations $\mathbf{\Phi}(\mathbf{q}) = \mathbf{0}$. Furthermore, if the joints are assumed frictionless, the work done by the constraint forces in a virtual (infinitesimal) displacement $d\mathbf{q}$ is zero, i.e.,

$$\mathbf{g}^{(c)^T} d\mathbf{q} = 0 \tag{2.70}$$

The Taylor series expansion of expression (2.43) about $\mathbf{q}$ is

$$\mathbf{\Phi}(\mathbf{q} + d\mathbf{q}) = \mathbf{\Phi}(\mathbf{q}) + \mathbf{\Phi}_q d\mathbf{q} \tag{2.71}$$

if the higher order terms in $d\mathbf{q}$ are ignored. Since the virtual displacement $d\mathbf{q}$ must be consistent with the constraints (expression (2.43)), it is required that

$$\mathbf{\Phi}(\mathbf{q} + d\mathbf{q}) = \mathbf{0} \tag{2.72}$$

Substituting expressions (2.43) and (2.72) into expression (2.71), yields

$$\mathbf{\Phi}_q d\mathbf{q} = \mathbf{0} \tag{2.73}$$

According to Nikravesh [65] the vector of n coordinates $\mathbf{q}$ may be partitioned into a set of m dependent coordinates $\mathbf{u}$ and a set of $n - m$ independent coordinates $\mathbf{v}$, i.e., $\mathbf{q} \equiv [\mathbf{u}^T, \mathbf{v}^T]^T$. This partitioning yields $d\mathbf{q} = [d\mathbf{u}^T, d\mathbf{v}^T]^T$, $\mathbf{\Phi}_q = [\mathbf{\Phi}_u, \mathbf{\Phi}_v]$ and $\mathbf{g}^{(c)} = \left[\mathbf{g}_{(u)}^{(c)^T}, \mathbf{g}_{(v)}^{(c)^T}\right]^T$.

Expression (2.70) may therefore be written as

$$\mathbf{g}_{(u)}^{(c)^T} d\mathbf{u} = -\mathbf{g}_{(v)}^{(c)^T} d\mathbf{v} \tag{2.74}$$

and from expression (2.73) it follows that

$$\mathbf{\Phi}_u d\mathbf{u} = -\mathbf{\Phi}_v d\mathbf{v} \tag{2.75}$$

Appending these two expressions to each other gives

$$\begin{bmatrix} \mathbf{g}_{(u)}^{(c)^T} \\ \boldsymbol{\Phi}_u \end{bmatrix} \mathbf{du} = -\begin{bmatrix} \mathbf{g}_{(v)}^{(c)^T} \\ \boldsymbol{\Phi}_v \end{bmatrix} \mathbf{dv} \tag{2.76}$$

Since $\boldsymbol{\Phi}_u$ is an $m \times m$ matrix with m independent rows, $\boldsymbol{\Phi}_u$ is a basis in R^m, and $\mathbf{g}_{(u)}^{(c)^T}$ may therefore be written as a linear combination of the m rows of $\boldsymbol{\Phi}_u$, i.e.,

$$\mathbf{g}_{(u)}^{(c)} = \boldsymbol{\Phi}_u^T \boldsymbol{\lambda} \tag{2.77}$$

where $\boldsymbol{\lambda}$ is a m-vector of multipliers known as *LaGrange multipliers.*

Substitution of expression (2.77) into expression (2.74) yields

$$\boldsymbol{\lambda}^T \boldsymbol{\Phi}_u \mathbf{du} = -\mathbf{g}_{(v)}^{(c)^T} \mathbf{dv} \tag{2.78}$$

and from expression (2.75) it follows that

$$-\boldsymbol{\lambda}^T \boldsymbol{\Phi}_v \mathbf{dv} = -\mathbf{g}_{(v)}^{(c)^T} \mathbf{dv} \tag{2.79}$$

Since vector $\mathbf{v}$ is independent, expression (2.79) must hold for an arbitrary virtual displacement $\mathbf{dv}$, which implies that

$$\mathbf{g}_{(v)}^{(c)} = \boldsymbol{\Phi}_v^T \boldsymbol{\lambda} \tag{2.80}$$

Furthermore, appending expressions (2.77) and (2.80) yields

$$\begin{bmatrix} \mathbf{g}_{(u)}^{(c)} \\ \mathbf{g}_{(v)}^{(c)} \end{bmatrix} = \begin{bmatrix} \boldsymbol{\Phi}_u^T \\ \boldsymbol{\Phi}_v^T \end{bmatrix} \boldsymbol{\lambda} \tag{2.81}$$

or simply

$$\mathbf{g}^{(c)} = \boldsymbol{\Phi}_q^T \boldsymbol{\lambda} \tag{2.82}$$

Finally substituting expression (2.82) into expression (2.69) gives the planar equations of motion for a system of constrained bodies, i.e.:

$$\mathbf{M}\ddot{\mathbf{q}} - \boldsymbol{\Phi}_q^T \boldsymbol{\lambda} = \mathbf{g} \tag{2.83}$$

Thus for a given vector of external forces $\mathbf{g}$, the *forward dynamic analysis* yields a unique solution for $\mathbf{q}$, $\dot{\mathbf{q}}$, $\ddot{\mathbf{q}}$ and $\boldsymbol{\lambda}$ when the constraint equations (2.43) are considered simultaneously with the differential equations of motion (2.83), and a proper set of initial conditions are specified.

2.6.3 Constraint reaction forces

The joint reaction forces given by expression (2.82) are studied here for the joints (kinematic pairs) of the planar Gough-Stewart platform.

2.6.3.1 Revolute joint

Consider the revolute joint connecting bodies 1 and 2 of the planar Gough-Stewart platform (see Figure 2.5). Figure 2.14 shows a schematic representation of the isolated revolute joint.

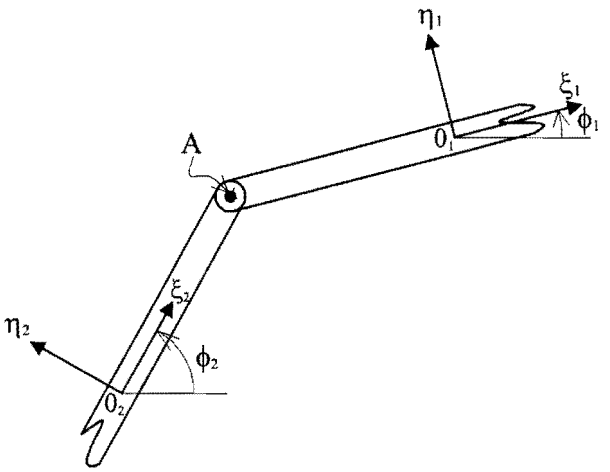

Figure 2.14: Revolute joint connecting bodies 1 and 2 of the planar Gough-Stewart platform.

The equations of motion of bodies 1 and 2 follow from expression (2.83), i.e.,

$$\mathbf{M}_1\ddot{\mathbf{q}}_1 - \mathbf{\Phi}_{\mathbf{q}_1}^{\mathrm{T}}\boldsymbol{\lambda} = \mathbf{g}_1 \tag{2.84}$$

and

$$\mathbf{M}_2\ddot{\mathbf{q}}_2 - \mathbf{\Phi}_{\mathbf{q}_2}^{\mathrm{T}}\boldsymbol{\lambda} = \mathbf{g}_2 \tag{2.85}$$

Using the applicable entries in the Jacobian matrix of the planar Gough-Stewart platform (see expression (2.62)), expression (2.84) may be written in expanded form:

$$\begin{bmatrix} m & & \\ & m & \\ & & \mu \end{bmatrix}_1 \begin{bmatrix} \ddot{x} \\ \ddot{y} \\ \ddot{\phi} \end{bmatrix}_1 - \begin{bmatrix} 1 & 0 \\ 0 & 1 \\ -\xi_1^A \sin\phi_1 & \xi_1^A \cos\phi_1 \end{bmatrix} \begin{bmatrix} \lambda_1 \\ \lambda_2 \end{bmatrix} = \begin{bmatrix} f_{(x)} \\ f_{(y)} \\ n \end{bmatrix}_1 \tag{2.86}$$

Expression (2.86) may be written as a set of three separate equations:

$$m_1\ddot{x}_1 = f_{(x)_1} + \lambda_1 \tag{2.87}$$

$$m_1\ddot{y}_1 = f_{(y)_1} + \lambda_2 \tag{2.88}$$

$$\mu_1\ddot{\phi}_1 = n_1 - (\xi_1^A \sin\phi_1)\lambda_1 + (\xi_1^A \cos\phi_1)\lambda_2 \tag{2.89}$$

Expression (2.87) indicates that besides the resultant external force $f_{(x)_1}$, another force λ_1 due to the constraints acts in the x-direction on body 1. Similarly, expression (2.88) indicates that besides external force $f_{(y)_1}$, another constraint force λ_2 acts in the y-direction on body 1. Figure 2.15 shows a free-body diagram of body 1, indicating constraint forces λ_1 and λ_2.

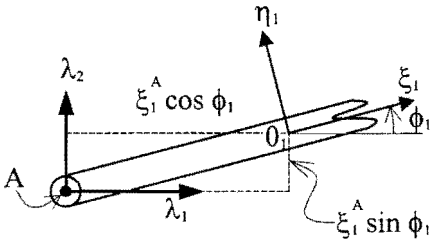

Figure 2.15: Free-body diagram of body 1 as part of the revolute joint with body 2.

The moment arm of λ_1 is $\xi_1^A \sin\phi_1$ with $\xi_1^A < 0$, which results in a positive moment $-(\xi_1^A \sin\phi_1)\lambda_1$ about 0_1 coinciding with the center of mass of body 1. Similarly, the moment arm of λ_2 is $\xi_1^A \cos\phi_1$ with $\xi_1^A < 0$, and therefore moment $(\xi_1^A \cos\phi_1)\lambda_2$ acts in the negative rotational direction.

Expression (2.85) may similarly be written in expanded form using the applicable entries in the Jacobian matrix (expression (2.62)):

$$\begin{bmatrix} m & & \\ & m & \\ & & \mu \end{bmatrix}_2 \begin{bmatrix} \ddot{x} \\ \ddot{y} \\ \ddot{\phi} \end{bmatrix}_2 - \begin{bmatrix} -1 & 0 \\ 0 & -1 \\ \xi_2^A \sin\phi_2 & -\xi_2^A \cos\phi_2 \end{bmatrix} \begin{bmatrix} \lambda_1 \\ \lambda_2 \end{bmatrix} = \begin{bmatrix} f_{(x)} \\ f_{(y)} \\ n \end{bmatrix}_2 \tag{2.90}$$

or

$$m_2\ddot{x}_2 = f_{(x)_2} - \lambda_1 \tag{2.91}$$

$$m_2\ddot{y}_2 = f_{(y)_2} - \lambda_2 \tag{2.92}$$

$$\mu_2\ddot{\phi}_2 = n_2 + (\xi_2^A \sin\phi_2)\lambda_1 - (\xi_2^A \cos\phi_2)\lambda_2 \tag{2.93}$$

Expressions (2.91) and (2.92) indicate that the constraint forces λ_1 and λ_2 respectively act in the negative x and y-directions on body 2. The corresponding free-body diagram of body 2 is shown in Figure 2.16.

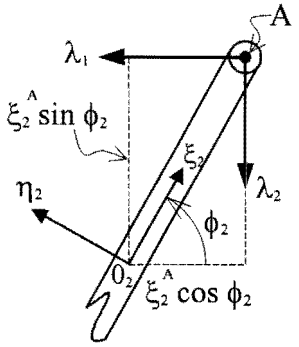

Figure 2.16: Free-body diagram of body 2 as part of the revolute joint with body 1.

From Figure 2.16 it follows that the moment arm of λ_1 is $\xi_2^A \sin\phi_2$ with $\xi_2^A > 0$, which yields a positive moment $(\xi_2^A \sin\phi_2)\lambda_1$ about 0_2 coinciding with the center of mass of body 2. Similarly, the moment arm of λ_2 is $\xi_2^A \cos\phi_2$ with $\xi_2^A > 0$, which gives a negative moment $-(\xi_2^A \cos\phi_2)\lambda_2$ about 0_2.

Note that the multipliers λ_1 and λ_2 can assume both positive and negative values. In any case, the reaction forces acting at the revolute joint on the connecting bodies are always equal in magnitude and mutually opposite in direction.

2.6.3.2 Translational joint

Consider the translational joint between bodies 2 and 5 of the planar Gough-Stewart platform. Figure 2.17 shows a schematic representation of the joint.

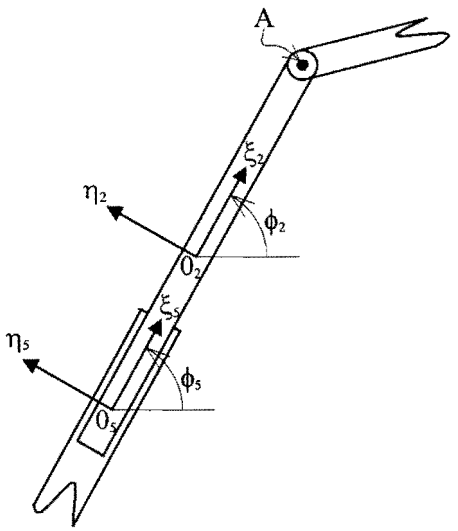

Figure 2.17: Translational joint between bodies 2 and 5 of the planar Gough-Stewart platform.

Following a similar argument as that outlined in Section 2.6.3.1, the equations of motion of body 2 may be written as:

$$\begin{bmatrix} m & & \\ & m & \\ & & \mu \end{bmatrix}_2 \begin{bmatrix} \ddot{x} \\ \ddot{y} \\ \ddot{\phi} \end{bmatrix}_2 - \begin{bmatrix} -\xi_2^A \sin\phi_2 & 0 \\ \xi_2^A \cos\phi_2 & 0 \\ (x_5 - x_2)\xi_2^A \cos\phi_2 + (y_5 - y_2)\xi_2^A \sin\phi_2 & -1 \end{bmatrix} \begin{bmatrix} \lambda_1 \\ \lambda_2 \end{bmatrix} = \begin{bmatrix} f_{(x)} \\ f_{(y)} \\ n \end{bmatrix}_2 \qquad (2.94)$$

or

$$m_2\ddot{x}_2 = f_{(x)_2} - \xi_2^A \sin\phi_2\lambda_1 \qquad (2.95)$$

$$m_2\ddot{y}_2 = f_{(y)_2} + \xi_2^A \cos\phi_2\lambda_1 \qquad (2.96)$$

$$\mu_2\ddot{\phi}_2 = n_2 + (x_5 - x_2)\xi_2^A \cos\phi_2\lambda_1 + (y_5 - y_2)(\xi_2^A \sin\phi_2)\lambda_1 - \lambda_2 \qquad (2.97)$$

The free-body diagram of body 2 is shown in Figure 2.18. Nikravesh [65] explains that the force associated with λ_1 is the reaction force caused by the constraint equation which eliminates relative motion between bodies 2 and 5 in a direction perpendicular to the line of translation. It is therefore expected, as can easily be proved, that this reaction force ($\vec{\mathbf{k}}_1$ in Figure 2.18) is perpendicular to the line of translation.

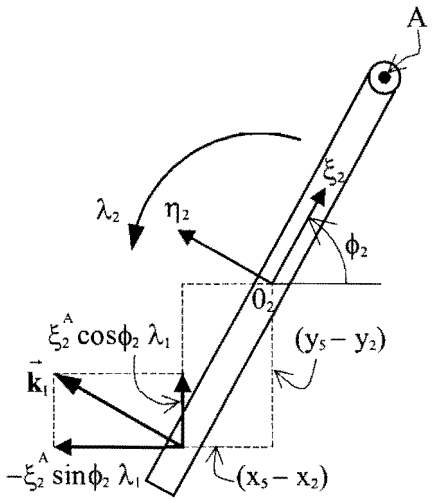

Figure 2.18: Free-body diagram of body 2 as part of the translational joint with body 5.

It follows from (2.97), and as shown in Figure 2.18, that the moment arm of the force $\xi_2^A \cos\phi_2\lambda_1$ about 0_2 is $(x_5 - x_2)$, and the moment arm of the force $-\xi_2^A \sin\phi_2\lambda_1$ is $(y_5 - y_2)$. For the orientation of body 2 shown in Figure 2.18, $(x_5 - x_2) < 0$ and $(y_5 - y_2) < 0$, from which it follows that both moments $(x_5 - x_2)\xi_2^A \cos\phi_2\lambda_1$ and $(y_5 - y_2)\xi_2^A \sin\phi_2\lambda_1$ are negative moments.

The contribution of the second constraint equation, which eliminates relative rotation between bodies 2 and 5, is a couple acting on body 2. Note that λ_2 may be a positive or negative quantity.

The equations of motion of body 5 are similarly given by

$$\begin{bmatrix} m & & \\ & m & \\ & & \mu \end{bmatrix}_5 \begin{bmatrix} \ddot{x} \\ \ddot{y} \\ \ddot{\phi} \end{bmatrix}_5 - \begin{bmatrix} \xi_2^A \sin\phi_2 & 0 \\ -\xi_2^A \cos\phi_2 & 0 \\ 0 & 1 \end{bmatrix} \begin{bmatrix} \lambda_1 \\ \lambda_2 \end{bmatrix} = \begin{bmatrix} f_{(x)} \\ f_{(y)} \\ n \end{bmatrix}_5 \tag{2.98}$$

or

$$m_5\ddot{x}_5 = f_{(x)_5} + \xi_2^A \sin\phi_2\lambda_1 \tag{2.99}$$

$$m_5\ddot{y}_5 = f_{(y)_5} - \xi_2^A \cos\phi_2\lambda_1 \tag{2.100}$$

$$\mu_5\ddot{\phi}_5 = n_5 - \lambda_2 \tag{2.101}$$

The corresponding free-body diagram of body 5 is shown in Figure 2.19. Note that $-\lambda_2$ is the only constraint moment acting on body 5.

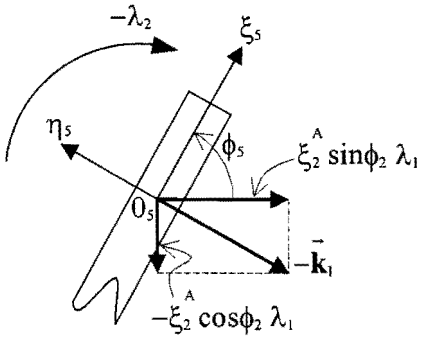

Figure 2.19: Free-body diagram of body 5 as part of the translational joint with body 2.

2.6.4 Vector of forces

The external force vector **g** in expression (2.83), contains all the external forces acting on the individual bodies of the system, i.e.,

$$\mathbf{g} = \left[\mathbf{g}_1^T, \mathbf{g}_2^T, \ldots, \mathbf{g}_b^T\right]^T \tag{2.102}$$

To construct the vector **g**, the external force vector for each body must be determined. For a typical body *i*, the external force vector $\mathbf{g}_i$ is

$$\mathbf{g}_i = [f_{(x)}, f_{(y)}, n]_i^T \tag{2.103}$$

where $f_{(x)i}$, $f_{(y)i}$ and n_i are respectively the sums of all force components in the x and y directions and the sum of all the moments respectively.

In the remainder of this sub-section, the two types of external forces that act on the planar Gough-Stewart platform are discussed, and their contribution to **g** determined.

2.6.4.1 Gravity

The first external force acting on the moving bodies that make up the planar Gough-Stewart platform is *gravity*. In accordance with Nikravesh [65], the direction of gravity is chosen to be in the negative y-direction. If w_i is the weight of the body *i*, i.e., $w_i = m_i g$, then the contribution of this force to the vector of force of body *i* is:

$$\mathbf{g}_i^{(\text{gravity})} = [0, -w, 0]_i^T \tag{2.104}$$

The first seven bodies of the planar Gough-Stewart platform in Figure 2.5, all have known weights contributing to the vector of external forces of each body, i.e., $\mathbf{g}_i^{(\text{gravity})} = [0,-w,0]_i^T$, for $i = 1,2,...,7$. Since the eighth body is the fixed ground, a zero weight is allocated to it, and a zero contribution is made to the vector of external force of body 8.

2.6.4.2 Single force

The second type of external force that acts on the planar Gough-Stewart platform is what Nikravesh [65] refers to as a *single force*. This is due to the fact that the planar Gough-Stewart platform is to be used as a machining center. For both machining centers with either a fixed workpiece or a fixed cutting tool, there is a contact force between the cutting tool and the workpiece. This contact force may be modeled as a single force.

Consider the general case, where a single force $\vec{\mathbf{f}}_i$ acts with a known direction at point P_i on body i as shown in Figure 2.20.

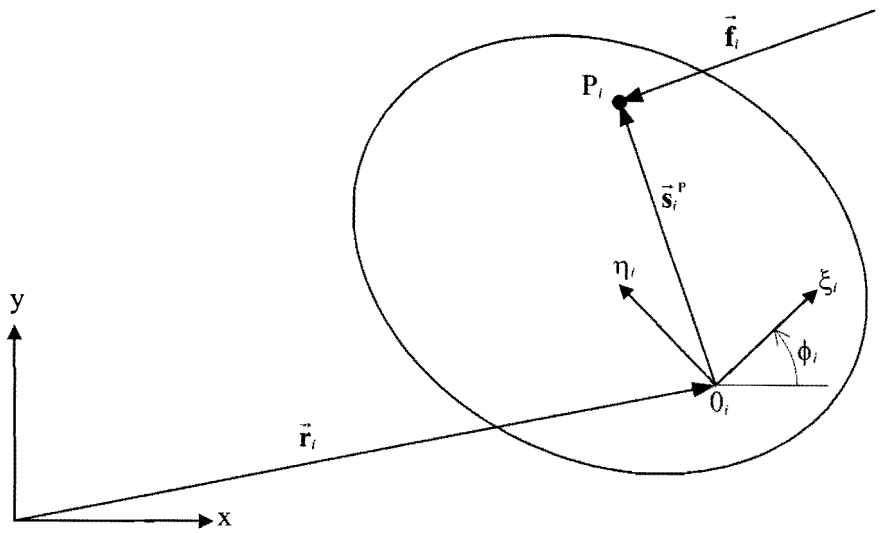

Figure 2.20: A body acted upon by a constant force (after [65]).

The force $\vec{\mathbf{f}}_i$ in the above figure has components $f_{(x)i}$ and $f_{(y)i}$. If the local coordinates of P_i are known as $\mathbf{s}_i'^P = [\xi^P, \eta^P]_i^T$, then the global coordinates of point P_i are given by $\mathbf{s}_i^P = \mathbf{A}_i \mathbf{s}_i'^P$ (see expression (2.1)). The moment of $\vec{\mathbf{f}}_i$ about 0_i, which coincides with the center of mass of body i is

$$\begin{aligned} n_i &= (\tilde{\mathbf{s}}_i^P \mathbf{f}_i)_{(z)} \\ &= -s_{(y)i}^P f_{(x)i} + s_{(x)i}^P f_{(y)i} \\ &= -(\xi_i^P \sin\phi_i + \eta_i^P \cos\phi_i) f_{(x)i} + (\xi_i^P \cos\phi_i - \eta_i^P \sin\phi_i) f_{(y)i} \end{aligned} \qquad (2.105)$$

Note that $\tilde{\mathbf{s}}_i^P$ represents the expansion of $\mathbf{s}_i^P$ into a skew-symmetric matrix (see expression (A.18) and [65]).

The contribution of this force to the vector of forces of body i is

$$\mathbf{g}_i^{(\text{single f})} = [\mathrm{f}_{(\mathrm{x})}, \mathrm{f}_{(\mathrm{y})}, \mathrm{n}]_i^{\mathrm{T}} \tag{2.106}$$

In particular, the contact force between the cutting tool and the workpiece may also be referred to as a *cutting force*. For both the fixed workpiece and fixed tool cases of the planar Gough-Stewart platform machining center, this cutting force contributes to the vector of forces of body 1 (the moving platform). The contribution of the cutting force to the vector of forces of body 1 is subsequently labeled as $\mathbf{g}_1^{(\text{cutting f})}$.

2.6.4.2.1 Fixed workpiece

The same assumptions as listed under Section 2.4.1, are made here, namely that at any given time instant it is assumed that the following are known:

1. the global position of the cutting tool tip (P in Figure 2.8) on the prescribed tool path, and
2. the angle β between the platform mounted tool and the normal to the tool path at the point of contact (see Figure 2.8) and measured positive in the CCW direction.

The free-body diagram of a typical fixed workpiece scenario is depicted in Figure 2.21. Since the cutting force is applied to body 1 it is designated by $\vec{\mathbf{f}}_1^{\,\text{cut}}$.

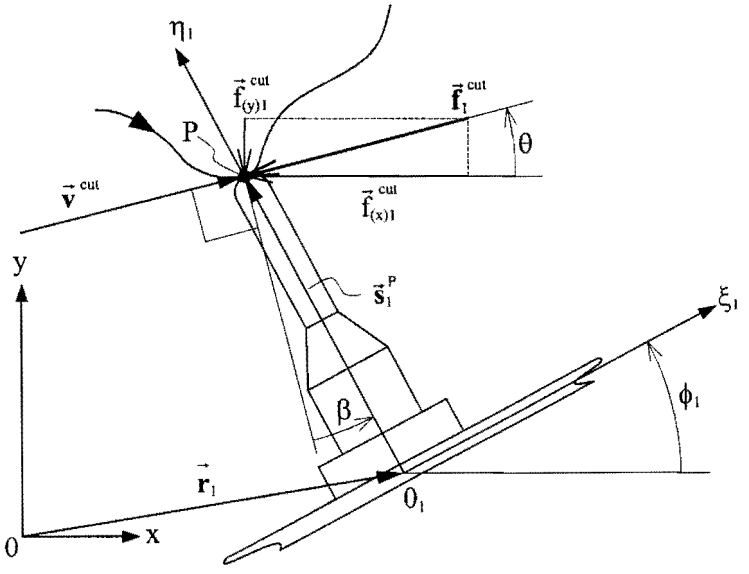

Figure 2.21: Free-body diagram for the fixed workpiece scenario.

The cutting force $\vec{\mathbf{f}}_1^{\,\text{cut}}$ is collinear with the tangent to the prescribed tool path at the point of contact, and it is modeled as a "resistance" force. This implies that the cutting force $\vec{\mathbf{f}}_1^{\,\text{cut}}$ is *oppositely* directed to the direction of travel, with magnitude assumed to be linearly dependent on the magnitude of tangential speed with which the prescribed tool path is traced $\left|\vec{\mathbf{v}}^{\,\text{cut}}\right|$.

It is assumed here that the vector $\vec{\mathbf{v}}^{cut}$ has a known magnitude and direction, which are calculated as will be described in **Chapter 3** (see also Section 2.5 expression (2.63)). With the magnitude of the cutting velocity $\left|\vec{\mathbf{v}}^{cut}\right|$ known, the magnitude of the cutting force is given by:

$$\left|\vec{\mathbf{f}}_1^{cut}\right| = \left|\vec{\mathbf{v}}^{cut}\right| C_{cut} \tag{2.107}$$

where C_{cut} is a "cutting force constant" expressed in $\frac{Ns}{m}$ as a positive quantity corresponding to the assumption made.

Vector $\vec{\mathbf{f}}_1^{cut}$ is represented in the global reference frame by $\mathbf{f}_1^{cut}$, i.e., $\vec{\mathbf{f}}_1^{cut} : \mathbf{f}_1^{cut} = [f_{(x)}^{cut}, f_{(y)}^{cut}]_1^T$. Similarly, vector $\vec{\mathbf{v}}^{cut}$ is represented in the global reference frame by $\mathbf{v}^{cut}$. Since the gradient angle θ is known at the point of contact, i.e., $\tan\theta = \frac{dy}{dx}$ (see expression (2.33)), the components of the cutting force as shown in Figure 2.21 are given by

$$f_{(x)1}^{cut} = -\left|\mathbf{f}_1^{cut}\right| \cos\theta \tag{2.108}$$

and

$$f_{(y)1}^{cut} = -\left|\mathbf{f}_1^{cut}\right| \sin\theta \tag{2.109}$$

The point of contact between the cutting tool and the workpiece is given by $\mathbf{s}_1'^{P} = \begin{bmatrix} 0 \\ \eta^P \end{bmatrix}_1$ as explained in Section 2.4.1. Hence the moment of $\vec{\mathbf{f}}_1^{cut}$ about the center of mass of body 1, n_1^{cut}, may be determined using expression (2.105), i.e.,

$$n_1^{cut} = -(\eta_1^P \cos\phi_1) f_{(x)1}^{cut} - (\eta_1^P \sin\phi_1) f_{(y)1}^{cut} \tag{2.110}$$

The validity of expression (2.110) may be verified by considering the situation depicted in the free-body diagram (Figure 2.21). It is clear that the x-component of the cutting force $f_{(x)1}^{cut}$ in Figure 2.21 is *negative*. The moment arm of $f_{(x)1}^{cut}$ is $\eta_1^P \cos\phi_1$. Thus, the first term in expression (2.110), $-(\eta_1^P \cos\phi_1) f_{(x)1}^{cut}$, yields a *positive* moment.

Similarly, the y-component of the cutting force $f_{(y)1}^{cut}$ in Figure 2.21 is *negative*, and the moment arm of $f_{(y)1}^{cut}$ is $\eta_1^P \sin\phi_1$. The second term of expression (2.110), $-(\eta_1^P \sin\phi_1) f_{(y)1}^{cut}$, therefore also yields a *positive* moment in expression (2.110).

For the fixed workpiece scenario, the contribution of the cutting force to the force vector of body 1, is

$$\mathbf{g}_1^{(\text{cutting f})} = [f_{(x)}^{cut}, f_{(y)}^{cut}, n^{cut}]_1^T \qquad (2.111)$$

where $f_{(x)1}^{cut}$ is given by expressions (2.108), $f_{(y)1}^{cut}$ is given by expressions (2.109), and n_1^{cut} is given by expression (2.110).

2.6.4.2.2 Fixed cutting tool

The same assumptions as listed in Section 2.4.2 apply here, i.e., at any time instant the following are assumed to be known:

1. the local position of the cutting tool tip (P in Figure 2.10) on the prescribed tool path, and
2. the angle β (measured positive CCW), from the normal to the tool path at the point of contact, to the vertical axis of the fixed cutting tool (see Figure 2.10).

The free-body diagram of a typical fixed cutting tool scenario is depicted in Figure 2.22. As in the case of the fixed workpiece, the cutting force is again applied to body 1 and designated by $\vec{f}_1^{cut}$.

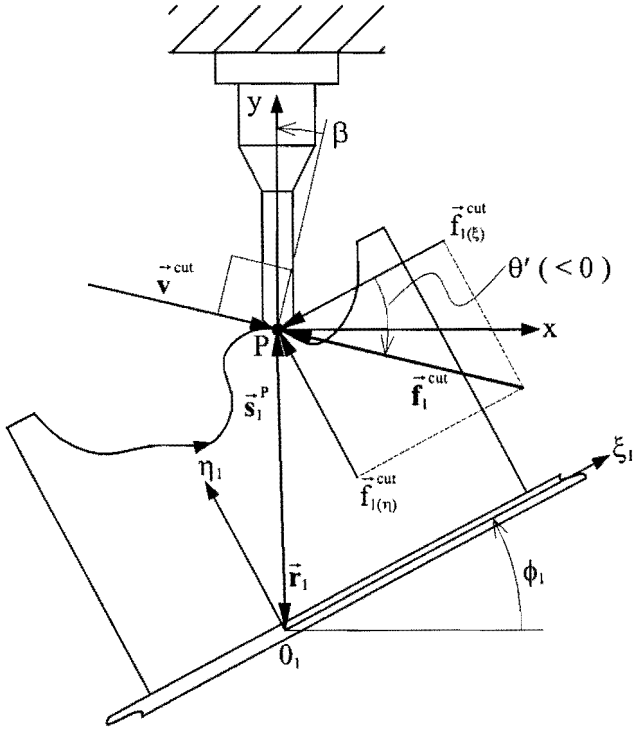

Figure 2.22: Free-body diagram for a fixed cutting tool scenario.

The modeling of the cutting force associated with the fixed cutting tool is done in a similar way to that done for the fixed workpiece.

In particular, the cutting force $\vec{f}_1^{cut}$ shown in Figure 2.22 is collinear with the tangent to the prescribed tool path at the point of contact. The tool path is specified in terms of the local $0_1\xi_1\eta_1$-coordinate

system. Furthermore, the direction of the cutting velocity $\vec{\mathbf{v}}^{cut}$ is also specified in terms of the local $0_1\xi_1\eta_1$-coordinate system ($\vec{\mathbf{v}}^{cut} : \mathbf{v}'^{cut} = [v^{cut}_{(\xi)}, v^{cut}_{(\eta)}]^T$) and the magnitude of the cutting velocity $\left|\mathbf{v}'^{cut}\right|$ is also assumed to be known (see **Chapter 3**).

Since the magnitude of the cutting force is again assumed to be linearly dependent on the magnitude of cutting velocity, expression (2.107) remains valid here, and the magnitude is therefore given by $\left|\vec{\mathbf{f}}_1^{cut}\right| = \left|\vec{\mathbf{v}}^{cut}\right| C_{cut}$.

The gradient angle of the prescribed tool path is known in terms of the local coordinates, $\tan\theta' = \dfrac{d\eta_1}{d\xi_1}$ (see expression (2.37)), hence the cutting force $\vec{\mathbf{f}}_1^{cut}$ may be represented in the local $0_1\xi_1\eta_1$ - coordinate system by $\vec{\mathbf{f}}_1^{cut} : \mathbf{f}_1'^{cut} = [f^{cut}_{(\xi)}, f^{cut}_{(\eta)}]^T_1$. The components of $\mathbf{f}_1'^{cut}$ are given by (see Figure 2.22)

$$f^{cut}_{(\xi)1} = -\left|\mathbf{f}_1'^{cut}\right| \cos\theta' \tag{2.112}$$

and

$$f^{cut}_{(\eta)1} = -\left|\mathbf{f}_1'^{cut}\right| \sin\theta' \tag{2.113}$$

The x- and y- components of the global cutting force representation $\vec{\mathbf{f}}_1^{cut} : \mathbf{f}_1^{cut} = [f^{cut}_{(x)}, f^{cut}_{(y)}]^T_1$ may be determined from the transformation given by expression (2.1):

$$f^{cut}_{(x)1} = f^{cut}_{(\xi)1} \cos\phi_1 - f^{cut}_{(\eta)1} \sin\phi_1 \tag{2.114}$$

and

$$f^{cut}_{(y)1} = f^{cut}_{(\xi)1} \sin\phi_1 + f^{cut}_{(\eta)1} \cos\phi_1 \tag{2.115}$$

or equivalently as

$$\mathbf{f}_1^{cut} = \mathbf{A}_1 \mathbf{f}_1'^{cut} \text{ with } A_1 = \begin{bmatrix} \cos\phi_1 & -\sin\phi_1 \\ \sin\phi_1 & \cos\phi_1 \end{bmatrix}$$

With the global components of the cutting force known, the moment of $\vec{\mathbf{f}}_1^{cut}$ about the center of mass of body 1 may be determined using expression (2.105). Note that this moment n_1^{cut} may also be determined using the local components of the cutting force, i.e.

$$\begin{aligned} n_1^{cut} &= (\tilde{\mathbf{s}}_1'^P \mathbf{f}_1'^{cut})_{(z)} \\ &= -\eta_1^P f^{cut}_{(\xi)1} + \xi_1^P f^{cut}_{(\eta)1} \end{aligned} \tag{2.116}$$

The validity of expression (2.116) is borne out by inspection of the free-body diagram depicted in Figure 2.22, from which it follows that the moment arm of $f^{cut}_{(\xi)1}$ is η_1^P. Since the ξ-component of the cutting

force in Figure 2.22 is directed in the negative ξ-direction, the term $-\eta_i^P f_{(\xi)i}^{cut}$ in expression (2.116) results in a positive moment. Similarly, the moment arm of $f_{(\eta)i}^{cut}$ is ξ_1^P, and since the η-component of the cutting force in Figure 2.22 is in the positive η-direction, the term $\xi_1^P f_{(\eta)1}^{cut}$ yields a positive moment.

For the fixed cutting tool scenario, the contribution of the cutting force to the external force vector of body 1 is:

$$\mathbf{g}_1^{(\text{cutting f})} = [f_{(x)}^{cut}, f_{(y)}^{cut}, n^{cut}]_1^T \tag{2.117}$$

where $f_{(x)1}^{cut}$ is given by expression (2.114), $f_{(y)1}^{cut}$ is given by expression (2.115) and n_1^{cut} is given by expression (2.116).

2.6.5 *Inverse dynamic analysis*

If the forces acting on a mechanical system are known, then the *equations of motion* can be solved to obtain the motion of the system [65]. This process is known as the *forward dynamic analysis*. In some problems, a specified motion for a mechanical system is sought and the objective is to determine the forces that must act on the system to produce such a motion. This process is usually referred to as *inverse dynamic* or *kinetostatic analysis*.

Haug [66] explains that inverse dynamic analysis is a hybrid form of kinematic and dynamic analysis in which the time history of positions or relative positions of one or more bodies in the system is prescribed, leading to complete determination of position, velocity, and acceleration of the system from the equations of kinematics. The equations of motion of the system are then solved, with known position, velocity, and acceleration, as algebraic equations to determine the forces that are required to generate the prescribed motion.

In general, for a system of constrained bodies with n coordinates and m independent constraint equations, the inverse dynamic analysis therefore requires k driving constraints of the form $\mathbf{\Phi}^{(d)} \equiv \mathbf{\Phi}(\mathbf{q}, t) = \mathbf{0}$ (see expression (2.44)) to be specified. The number of driving constraints to be specified is equal to the number of degrees of freedom of the system, i.e. $k = n - m$ (see expression (2.26)).

The three driving constraints of the planar Gough-Stewart platform under consideration have already been dealt with in Section 2.4. These constraints uniquely define the motion of body 1 (the moving platform) of the planar Gough-Stewart platform along a prescribed path.

Section 2.5 shows how the inverse kinematic analysis of the planar Gough-Stewart platform is done using the method of appended driving constraints. The inverse kinematic analysis yields the positions $\mathbf{q}$, velocities $\dot{\mathbf{q}}$ and accelerations $\ddot{\mathbf{q}}$ at each time instant as the prescribed path is traced.

The objective of this sub-section is to determine the three actuator forces required to move the moving platform along the prescribed path. For this purpose the equations of motion of a system of constrained bodies (expression (2.83)) are rewritten to include the unknown forces, i.e.,

$$\mathbf{M}\ddot{\mathbf{q}} - \boldsymbol{\Phi}_{\mathbf{q}}^{\mathrm{T}}\boldsymbol{\lambda} = \mathbf{g}^{(k)} + \mathbf{g}^{(u)} \tag{2.118}$$

where $\mathbf{g}^{(k)}$ is the vector of *known* forces (see expression (2.102)), and $\mathbf{g}^{(u)}$ is the vector of *unknown* forces. Expression (2.118) may be rewritten as

$$\mathbf{M}\ddot{\mathbf{q}} - \boldsymbol{\Phi}_{\mathbf{q}}^{\mathrm{T}}\boldsymbol{\lambda} - \mathbf{g}^{(u)} = \mathbf{g}^{(k)} \tag{2.119}$$

The unknown actuator forces are designated by $\vec{\mathbf{f}}_1$, $\vec{\mathbf{f}}_2$ and $\vec{\mathbf{f}}_3$, and respectively act on bodies 2, 3 and 4 as shown in Figure 2.23. By Newton's third law, for each force there is an equal and opposite reaction force. Hence, reaction forces $-\vec{\mathbf{f}}_1$, $-\vec{\mathbf{f}}_2$ and $-\vec{\mathbf{f}}_3$, respectively act on bodies 5, 6 and 7 and are also shown in the schematic Figure 2.23.

In particular, the lines of action of forces $\vec{\mathbf{f}}_1$ and $-\vec{\mathbf{f}}_1$ coincide with the line of translation of the translational joint between bodies 2 and 5. Similarly, the lines of action of forces $\vec{\mathbf{f}}_2$ and $-\vec{\mathbf{f}}_2$ coincide with the common line of translation of the translational joint between bodies 3 and 6, and the lines of action of forces $\vec{\mathbf{f}}_3$ and $-\vec{\mathbf{f}}_3$ coincide with the common line of translation of bodies 4 and 7.

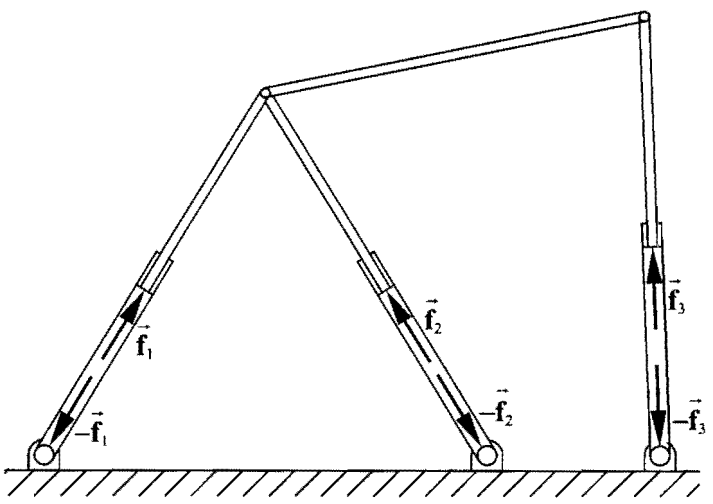

Figure 2.23: Unknown actuator forces of the planar Gough-Stewart platform.

Figure 2.24 shows the free-body diagram of body 2 with the unknown actuator force $\vec{\mathbf{f}}_1$ applied to the body, as well as the constraint force $\vec{\mathbf{k}}_1$ and constraint moment λ_2 as a result of the translational coupling between bodies 2 and 5.

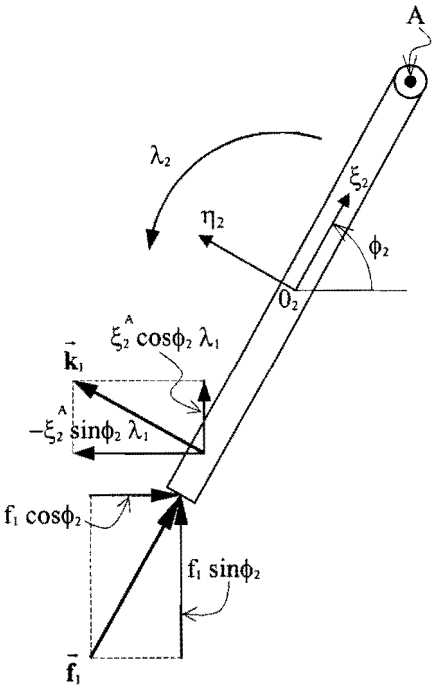

Figure 2.24: Free-body diagram of body 2 with the applied unknown actuator force $\vec{\mathbf{f}}_1$.

From expression (2.119) it follows that the equations of motion of body 2 are given by:

$$\begin{bmatrix} m & & \\ & m & \\ & & \mu \end{bmatrix}_2 \begin{bmatrix} \ddot{x} \\ \ddot{y} \\ \ddot{\phi} \end{bmatrix}_2 - \begin{bmatrix} -\xi_2^A \sin\phi_2 & 0 \\ \xi_2^A \cos\phi_2 & 0 \\ \begin{Bmatrix} (x_5 - x_2)\xi_2^A \cos\phi_2 \\ +(y_5 - y_2)\xi_2^A \sin\phi_2 \end{Bmatrix} & -1 \end{bmatrix} \begin{bmatrix} \lambda_1 \\ \lambda_2 \end{bmatrix} - \begin{bmatrix} f_1 \cos\phi_2 \\ f_1 \sin\phi_2 \\ 0 \end{bmatrix} = \begin{bmatrix} f_{(x)} \\ f_{(y)} \\ n \end{bmatrix}_2 \qquad (2.120)$$

where $f_1 > 0$ indicates that force $\vec{\mathbf{f}}_1$ is a "push-force" as chosen in Figure 2.24. Should the solution of expression (2.120) yield that $f_1 < 0$, then force $\vec{\mathbf{f}}_1$ actually is a "pull-force" acting in the opposite direction. Also note that actuator force $\vec{\mathbf{f}}_1$ does not cause a couple about the center of mass of body 2.

Expression (2.120) may also be written as

$$\begin{bmatrix} m & & \\ & m & \\ & & \mu \end{bmatrix}_2 \begin{bmatrix} \ddot{x} \\ \ddot{y} \\ \ddot{\phi} \end{bmatrix}_2 - \begin{bmatrix} -\xi_2^A \sin\phi_2 & 0 & \cos\phi_2 \\ \xi_2^A \cos\phi_2 & 0 & \sin\phi_2 \\ \begin{Bmatrix} (x_5 - x_2)\xi_2^A \cos\phi_2 \\ +(y_5 - y_2)\xi_2^A \sin\phi_2 \end{Bmatrix} & -1 & 0 \end{bmatrix} \begin{bmatrix} \lambda_1 \\ \lambda_2 \\ f_1 \end{bmatrix} = \begin{bmatrix} f_{(x)} \\ f_{(y)} \\ n \end{bmatrix}_2 \qquad (2.121)$$

With regard to the reaction force $-\vec{\mathbf{f}}_1$, Figure 2.25 shows the free-body diagram of body 5 with the unknown reaction force $-\vec{\mathbf{f}}_1$ applied to the body, as well as the constraint force $-\vec{\mathbf{k}}_1$ and constraint moment $-\lambda_2$ as a result of the translational coupling between bodies 2 and 5.

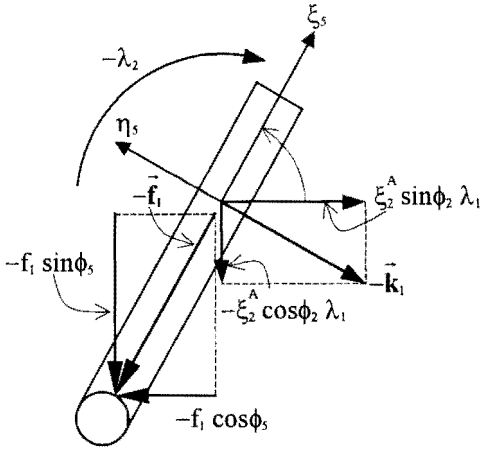

Figure 2.25: Free-body diagram of body 5 with the applied unknown reaction force $-\vec{\mathbf{f}}_1$.

From expression (2.119) it follows that the equations of motion of body 5 are given by:

$$\begin{bmatrix} m & & \\ & m & \\ & & \mu \end{bmatrix}_5 \begin{bmatrix} \ddot{x} \\ \ddot{y} \\ \ddot{\phi} \end{bmatrix}_5 - \begin{bmatrix} \xi_2^A \sin\phi_2 & 0 \\ -\xi_2^A \cos\phi_2 & 0 \\ 0 & 1 \end{bmatrix} \begin{bmatrix} \lambda_1 \\ \lambda_2 \end{bmatrix} - \begin{bmatrix} -f_1 \cos\phi_2 \\ -f_1 \sin\phi_2 \\ 0 \end{bmatrix} = \begin{bmatrix} f_{(x)} \\ f_{(y)} \\ n \end{bmatrix}_5 \qquad (2.122)$$

where $f_1 < 0$ indicates that the reaction force $-\vec{\mathbf{f}}_1$ is a "push reaction force" as chosen in Figure 2.25. Should the solution of expression (2.122) yield that $f_1 > 0$, the associated reaction force $-\vec{\mathbf{f}}_1$ actually is a "pull reaction force" acting in the opposite direction. Note that there is no couple about the center of mass of body 5.

Expression (2.120) may also be written as

$$\begin{bmatrix} m & & \\ & m & \\ & & \mu \end{bmatrix}_5 \begin{bmatrix} \ddot{x} \\ \ddot{y} \\ \ddot{\phi} \end{bmatrix}_5 - \begin{bmatrix} \xi_2^A \sin\phi_2 & 0 & -\cos\phi_2 \\ -\xi_2^A \cos\phi_2 & 0 & -\sin\phi_2 \\ 0 & 1 & 0 \end{bmatrix} \begin{bmatrix} \lambda_1 \\ \lambda_2 \\ f_1 \end{bmatrix} = \begin{bmatrix} f_{(x)} \\ f_{(y)} \\ n \end{bmatrix}_5 \qquad (2.123)$$

Similar expressions are also obtained for bodies 3 and 6, as well as bodies 4 and 7. Hence, the equations of motion of the total planar Gough-Stewart platform system may be written as:

$$\mathbf{M}\ddot{\mathbf{q}} - \begin{bmatrix} \boldsymbol{\Phi}_{\mathbf{q}}^{\mathrm{T}} & \mathbf{B} \end{bmatrix} \begin{bmatrix} \boldsymbol{\lambda} \\ \mathbf{ff} \end{bmatrix} = \mathbf{g}^{(k)} \qquad (2.124)$$

where $\mathbf{M}$ is a constant diagonal matrix, i.e. $\mathbf{M} = \mathrm{diag}[m_1, m_1, \mu_1, m_2, m_2, \mu_2, \ldots, m_8, m_8, \mu_8]$,

$\ddot{\mathbf{q}}$ is the acceleration vector $\ddot{\mathbf{q}} = [\ddot{x}_1, \ddot{y}_1, \ddot{\phi}_1, \ddot{x}_2, \ddot{y}_2, \ddot{\phi}_2, \ldots, \ddot{x}_8, \ddot{y}_8, \ddot{\phi}_8]^{\mathrm{T}}$,

$\boldsymbol{\Phi}_{\mathbf{q}}$ consist of the first 21 rows of the Jacobian matrix $\mathbf{J}$(see expression (2.62)),

B is the following 24×3 matrix:

$$\mathbf{B} = \begin{bmatrix} 0 & 0 & 0 & \cos\phi_2 & \sin\phi_2 & 0 & 0 & 0 & 0 & 0 & 0 & 0 & -\cos\phi_5 & -\sin\phi_5 & 0 & 0 & 0 & 0 & 0 & 0 & 0 & 0 & 0 & 0 \\ 0 & 0 & 0 & 0 & 0 & 0 & \cos\phi_3 & \sin\phi_3 & 0 & 0 & 0 & 0 & 0 & 0 & 0 & -\cos\phi_6 & -\sin\phi_6 & 0 & 0 & 0 & 0 & 0 & 0 & 0 \\ 0 & 0 & 0 & 0 & 0 & 0 & 0 & 0 & 0 & \cos\phi_4 & \sin\phi_4 & 0 & 0 & 0 & 0 & 0 & 0 & 0 & -\cos\phi_7 & -\sin\phi_7 & 0 & 0 & 0 & 0 \end{bmatrix}^T,$$

$\boldsymbol{\lambda}$ is a 21-vector containing the LaGrange multipliers, i.e., $\boldsymbol{\lambda} = [\lambda_1, \lambda_2, \lambda_3, ..., \lambda_{21}]^T$,

ff is the vector containing the magnitudes of the unknown actuator forces $\mathbf{ff} = [f_1 \quad f_2 \quad f_3]^T$ using the positive sign convention chosen in Figure 2.24, and

$\mathbf{g}^{(k)}$ is the vector of known external forces given acting on the planar Gough-Stewart platform

$$\mathbf{g}^{(k)} = \left[\left(\mathbf{g}_1^{(\text{gravity})} + \mathbf{g}_1^{(\text{cutting f})}\right)^T, \mathbf{g}_2^{(\text{gravity})T}, \mathbf{g}_3^{(\text{gravity})T}, \mathbf{g}_4^{(\text{gravity})T}, \mathbf{g}_5^{(\text{gravity})T}, \mathbf{g}_6^{(\text{gravity})T}, \mathbf{g}_7^{(\text{gravity})T}, 0, 0, 0\right]^T$$

The cutting force $\mathbf{g}_1^{(\text{cutting f})}$ is either given by expression (2.111) or expression (2.117) depending on the particular machining scenario, and finally expression (2.124) may be solved using a linear solver as explained in Section 2.5, to find the 24-vector $\begin{bmatrix} \boldsymbol{\lambda} \\ \mathbf{ff} \end{bmatrix}$.

2.7 Verification of special purpose program

In this section, the special-purpose program for analyzing the planar Gough-Stewart platform machining center is, tested and verified.

2.7.1 Jacobian matrix verification

The Jacobian matrix derived for the planar Gough-Stewart platform (expression (2.62)), is of importance, since it is used in both the inverse kinematic analysis of the mechanism and the inverse dynamic analysis. In order to verify the correctness of the Jacobian matrix constructed here, and to be used in the special purpose program, the general purpose **K**inematic **A**nalysis **P**rogram (**KAP**) developed by Nikravesh [65] is applied to do the inverse kinematic analysis of a specific planar Gough-Stewart platform following the simple test trajectory shown in Figure 2.26.

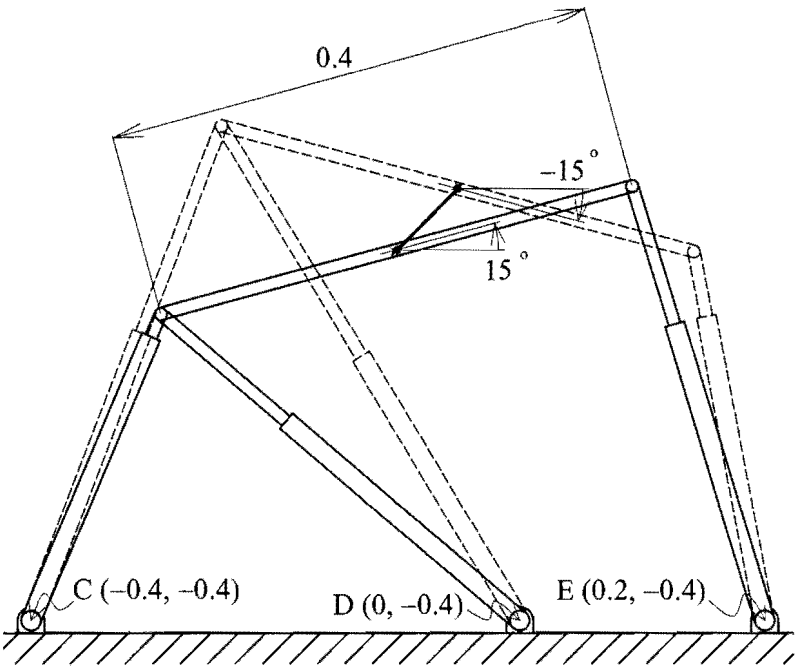

Figure 2.26: Straight line motion.

The length of the moving platform is chosen as 0.4 m, and the coordinates of the lower rotational joints C, D and E are as indicated in Figure 2.26.

Three independent driving constraints of the form given by expressions (2.27) - (2.29) prescribe the motion of the planar Gough-Stewart platform. In particular, for the simple straight line trajectory shown in Figure 2.26, expressions (2.27), (2.28) and (2.29) are respectively:

$$\Phi^{(d-1,1)} \equiv x_1 + 0.1 - 0.05t^2 = 0 \qquad (2.125)$$

$$\Phi^{(d-2,1)} \equiv y_1 + 0.1 - 0.05t^2 = 0 \qquad (2.126)$$

$$\Phi^{(d-3,1)} \equiv \phi_1 - \frac{\pi}{12} + \frac{\pi}{6}t^2 = 0 \qquad (2.127)$$

Driving constraints (2.125) and (2.126) control the displacement of the center of the moving platform (body 1 in Figure 2.5) in the x-y plane along a straight line from $(-0.1, -0.1)$ at $t = 0$, to $(-0.05, -0.05)$ at $t = 1\,s$. Driving constraint (2.127) controls the rotation of the moving platform from its initial orientation $\phi_1 = 15°$ at $t = 0$, to its final orientation $\phi_1 = -15°$ at $t = 1\,s$.

The results obtained by KAP [65] for the velocities and accelerations of the seven moving bodies are in exact agreement with the results obtained using expressions (2.51) and (2.56), indicating that the Jacobian matrix of the planar Gough-Stewart platform constructed here (expression (2.62)) is correct.

Furthermore, the analytical solution of the positions and orientations of the 7 bodies obtained from expressions (2.57) - (2.61) is also in exact agreement with the iterative solution obtained using KAP.

2.7.2 *Inverse dynamic analysis verification*

The objective of this sub-section is to verify the methodology for determining the unknown actuator forces as explained in Section 2.6.5.

The verification of expression (2.124) is done noting that it may also be used to determine the *static* balance forces required to support the planar Gough-Stewart platform in static equilibrium. It follows that with the planar Gough-Stewart platform in static equilibrium, $\ddot{\mathbf{q}} = \mathbf{0}$, and therefore expression (2.124) reduces to:

$$-\begin{bmatrix}\boldsymbol{\Phi}_{\mathbf{q}}^{\mathrm{T}} & \mathbf{B}\end{bmatrix}\begin{bmatrix}\boldsymbol{\lambda}\\ \mathbf{ff}\end{bmatrix} = \mathbf{g}^{(k)} \tag{2.128}$$

As explained in Sections 2.4 and 2.5, by prescribing the three driving constraints (expressions (2.27) - (2.29)) at any specific time instant, the Jacobian matrix given by expression (2.62) is uniquely defined. Therefore for any given stationary platform configuration, equation (2.128) may be solved for the vector $\begin{bmatrix}\boldsymbol{\lambda}\\ \mathbf{ff}\end{bmatrix}$ using a linear solver.

In expression (2.128):

$\boldsymbol{\Phi}_{\mathbf{q}}$ consist of the first 21 rows of the Jacobian matrix **J**(see expression (2.62)),

$$\mathbf{B} = \begin{bmatrix} 0 & 0 & 0 & \cos\phi_2 & \sin\phi_2 & 0 & 0 & 0 & 0 & 0 & 0 & 0 & -\cos\phi_5 & -\sin\phi_5 & 0 & 0 & 0 & 0 & 0 & 0 & 0 & 0 & 0 & 0 \\ 0 & 0 & 0 & 0 & 0 & 0 & \cos\phi_3 & \sin\phi_3 & 0 & 0 & 0 & 0 & 0 & 0 & 0 & -\cos\phi_6 & -\sin\phi_6 & 0 & 0 & 0 & 0 & 0 & 0 & 0 \\ 0 & 0 & 0 & 0 & 0 & 0 & 0 & 0 & 0 & \cos\phi_4 & \sin\phi_4 & 0 & 0 & 0 & 0 & 0 & 0 & 0 & -\cos\phi_7 & -\sin\phi_7 & 0 & 0 & 0 & 0 \end{bmatrix}^{\mathrm{T}},$$

$\boldsymbol{\lambda}$ is a 21-vector containing the LaGrange multipliers, i.e., $\boldsymbol{\lambda} = [\lambda_1, \lambda_2, \lambda_3, ..., \lambda_{21}]^{\mathrm{T}}$, and

$\mathbf{g}^{(k)} = \left[\mathbf{g}_1^{(k)\mathrm{T}}, \mathbf{g}_2^{(k)\mathrm{T}}, ..., \mathbf{g}_8^{(k)\mathrm{T}}\right]^{\mathrm{T}}$.

Consider the simple test example shown in Figure 2.27, where the vector of external forces is reduced to $\mathbf{g}^{(k)} = [1600, -440, 250, 0, 0, 0, ..., 0]^{\mathrm{T}}$.

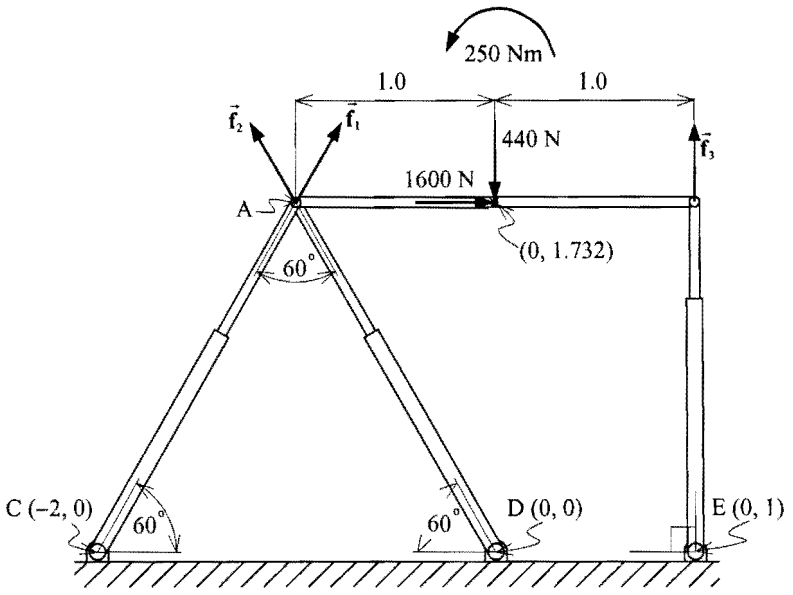

Figure 2.27: Simplified static analysis example.

The results obtained for the unknown actuator forces **ff** by solving expression (2.128) are $f_1 = -1400.8\,\text{N}$, $f_2 = 1799.2\,\text{N}$ and $f_3 = 95\,\text{N}$.

For this simple problem the unknown actuator force f_3 may also be obtained by considering the sum of the moments about A, i.e.: $\sum M_A = 0:\ 250 - 440 + 2f_3 = 0$ and thus $f_3 = 95\,\text{N}$.

Also, summing the external forces in the x- and y-directions and substituting the value for f_3 yields the following equations in the unknown actuator forces f_1 and f_2:

$$\sum F_x = 0: \quad f_1 \cos 60^\circ - f_2 \cos 60^\circ + 1600 = 0 \tag{2.129}$$

$$\sum F_y = 0: \quad f_1 \sin 60^\circ + f_2 \sin 60^\circ + f_3 - 440 = 0 \tag{2.130}$$

Solving (2.129) and (2.130) finally gives $f_1 = -1400.8\,\text{N}$ and $f_2 = 1799.2\,\text{N}$. This together with the value of $f_3 = 95\,\text{N}$ confirms the accuracy of the results obtained via (2.128).

2.7.3 *Fixed workpiece vs. fixed tool verification*

The two modes of operation of the machining center are explained in Sections 2.4.1 and 2.4.2. The objective of this section is to verify the actuator force computations, by reconciling the results for the fixed tool scenario with that of the fixed workpiece scenario. This is done by considering the case where the respective tool path specifications are such that the space path of the platform is identical for both scenarios.

For this illustrative example the fixed workpiece scenario is as depicted in Figure 2.28, and the cutting tool is omitted from the moving platform.

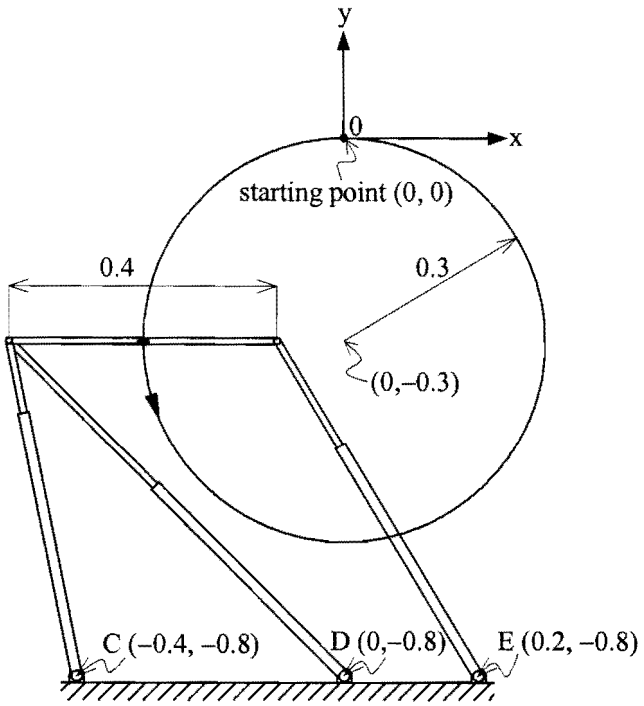

Figure 2.28: Fixed workpiece scenario with prescribed circular path.

The center of mass of the moving platform (body 1 in Figure 2.5) is controlled to trace the circle defined by

$$x^2 + (y + 0.3^2) = 0.3^2 \tag{2.131}$$

at a constant tangential speed of $0.1\,\mathrm{m/s}$.

This circle is traced in a CCW sense starting at $(x,y) = (0,0)$. It is furthermore required that the prescribed circular path be traced while a horizontal orientation is maintained by the moving platform, i.e. $\phi_1 \equiv 0$.

With the positional driving constraints and the fixed orientation prescribed, the inverse kinematic analysis may be done to obtain the acceleration vector $\ddot{\mathbf{q}} = [\ddot{\mathbf{q}}_1^T, \ddot{\mathbf{q}}_2^T, ..., \ddot{\mathbf{q}}_8^T]^T$ for any time instant. It is then used in the inverse dynamic analysis, which is done via the equations of motion given by expression (2.124).

The following mass matrix is used for the example planar Gough-Stewart platform shown in Figure 2.28:

$$\mathbf{M} = \mathrm{diag}[\mathbf{M}_1^T, \mathbf{M}_2^T, \mathbf{M}_3^T, ..., \mathbf{M}_8^T] \tag{2.132}$$

with

$$\mathbf{M}_1 = [3, 3, 0.0625]^T$$

$$\mathbf{M}_2 = \mathbf{M}_3 = \mathbf{M}_4 = [0.6, 0.6, 0.02]^T$$

$$\mathbf{M}_5 = \mathbf{M}_6 = \mathbf{M}_7 = [2.5, 2.5, 0.003]^T$$

$$\mathbf{M}_8 = [0, 0, 0]^T$$

and specified in SI units.

Figure 2.29 shows the computed actuator forces required to control the planar Gough-Stewart platform along the prescribed circular path at the specified constant tangential speed of 0.1 m/s. The cutting force, discussed in Section 2.6.4.2.1, is neglected here.

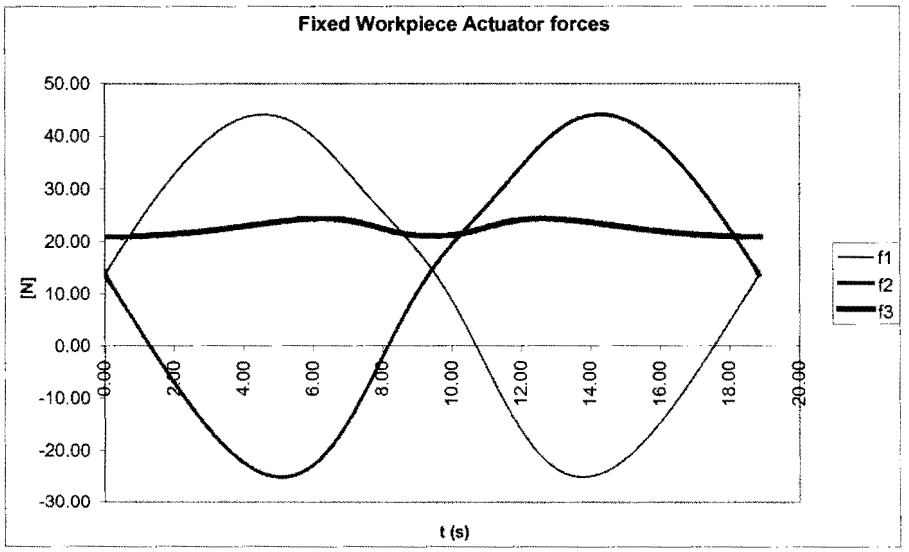

Figure 2.29: Actuator forces for the fixed workpiece circular tool path.

For the fixed tool scenario to be consistent with that of the fixed workpiece scenario, it is required to specify a prescribed path in the moving workpiece such that the motion in space of the moving platform is identical to the motion of the moving platform associated with the fixed workpiece example shown in Figure 2.28. For this to be so, the fixed cutting tool has to trace the prescribed solid circular path shown in Figure 2.30 in a CCW manner starting at $(\xi_1, \eta_1) = (0,0)$.

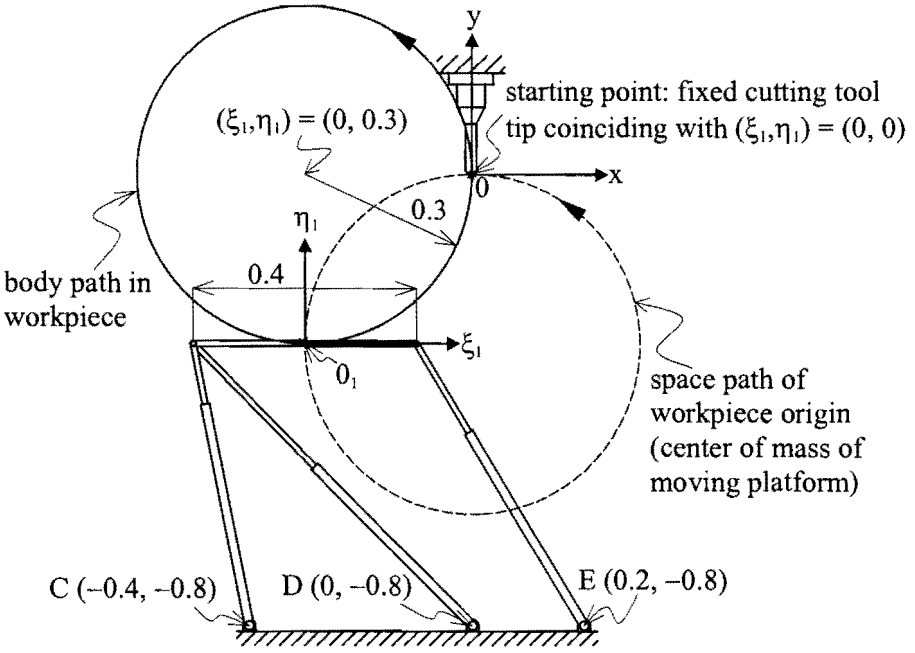

Figure 2.30: Fixed tool scenario with prescribed circular path.

In particular, the circular path in the local platform coordinate frame is defined by

$$\xi_1^{\,2} + (\eta_1 - 0.3^2) = 0.3^2 \qquad (2.133)$$

The global coordinate system is shown with its origin coinciding with the cutting tool tip. Using the transformations given by expressions (2.41) and (2.42), the motion of the moving platform in the global reference frame can be computed. This path is shown by the dashed circle in Figure 2.30 and corresponds exactly to the motion of the moving platform associated with the fixed workpiece example shown in Figure 2.28. Figure 2.31 shows the computed actuator forces required to manipulate the moving platform along the prescribed path of Figure 2.30. As is expected they are in exact agreement with the actuator forces shown in Figure 2.29. Note again that the cutting forces, discussed in Section 2.6.4.2.2, are neglected here to ensure that the load conditions are equivalent for both scenarios. This allows for a comparison of results. The fact that the results are identical gives further confidence in the respective methods of analysis.

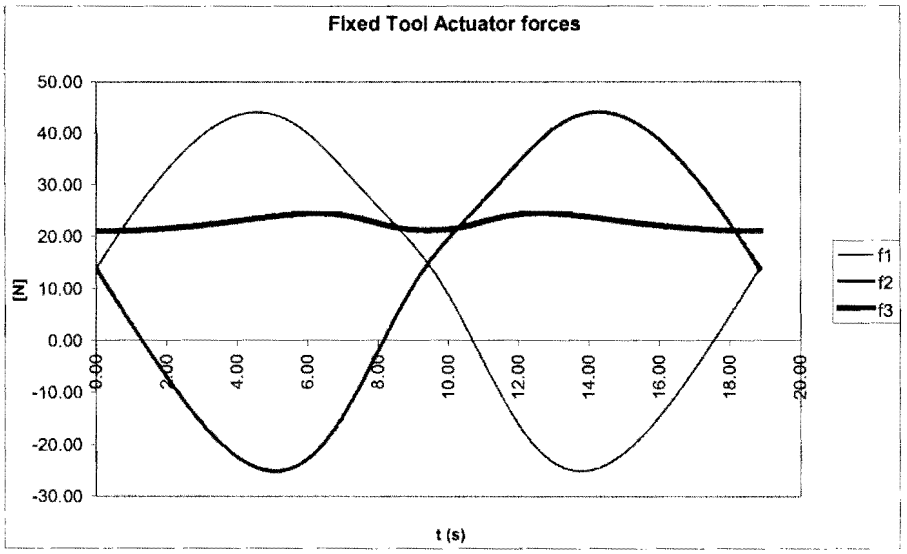

Figure 2.31: Actuator forces for the fixed tool circular tool path.